APPLICATION OF A MULTI-HYDROPHONE DRIFTER AND PORPOISE DETECTION SOFTWARE FOR MONITORING ATLANTIC HARBOUR PORPOISE (*PHOCOENA PHOCOENA*) ACTIVITY IN AND NEAR MINAS PASSAGE

by

Michael J. Adams

Thesis submitted in partial fulfillment of the

requirements for the Degree of

Bachelor of Science with

Honours in Biology

Acadia University

April, 2018

This thesis by Michael J. Adams

is accepted in its present form by the

Department of Biology

as satisfying the thesis requirements for the degree of

Bachelor of Science with Honours

Approved by the Thesis Supervisors

_____ _____

Dr. Anna Redden Date

_____ _____

Dr. Brian Sanderson Date

Approved by the Head of the Department

_____ _____

Dr. Brian Wilson Date

Approved by the Chair of the Honours Committee

_____ _____

Dr. Matthew Lukeman Date

_____

Signature of Author

_____

Date

ACKNOWLEDGEMENTS

I would like to thank my supervisors, Dr. Anna Redden and Dr. Brian Sanderson for their support, insight and instruction during this project and thesis preparation. Dr. Redden's experience in the organization of scientific studies and the preparation of academic publications was an invaluable asset over the course of this experience. Her continued support and encouragement of my academic pursuits was a crucial factor in my success academically. The important investment of Dr. Sanderson's time and effort was deeply appreciated throughout my work on this project. His willingness to impart to me his knowledge of physics, data analysis, and computer programming was key to the completion of my thesis and will remain tools that I will carry for the rest of my life.

I would also like to thank Randy Corcoran, whose interest and enthusiasm for the work being done, as well as his expertise navigating the waters of Minas Passage, made this project possible. Thanks also goes to the Ocean Sonics team for their technical advice and equipment support. Additionally, I would like to thank my lab mate, Mark Billard, for being a great first resource whenever I had a question. I thank Acadia University and the Acadia Centre for Estuarine Research for providing funding and materials for this project, as well as the George Baker Tidal Energy and Environment Scholarship and the Blomidon Naturalist Society for funding towards my studies.

Finally, I would like to thank my friends and family for their support and encouragement over the course of this project. Special thanks to Kristen, for her unwavering support and for reminding me to take a break every now and then.

TABLE OF CONTENTS

LIST OF TABLES

LIST OF FIGURES

LIST OF ABBREVIATIONS AND SYMBOLS

a	acceleration
A_n	cosine part of discrete Fourier transform
B_n	sine part of discrete Fourier transform
c	speed of sound in water (1500 m/s)
CLA	Crown Lease Area
cm	Centimeter
COSEWIC	Committee on the Status of Endangered Wildlife in Canada
CPOD	Chelonia Porpoise Detector
CW	Constant wave
dB	Decibel
DFT	Discrete Fourier Transform
DPM	Detection Positive Minute (value 0 or 1)
Eq.	Equation
F	force
f	frequency
FFT	Fast Fourier Transform
FORCE	Fundy Ocean Research Center for Energy
GAM	Generalized Additive Model
GB	Giga-byte
GEE	Generalized Estimating Equation
GPS	Global Positioning System
H	Horizontal
Hz	Hertz
ICI	Inter Click Interval
k	0, 1, 2, 3, …, N-1
kg	Kilogram
kHz	Kilohertz
kJ	Kilojoule
km	Kilometer
I	Intensity
l	wavelength
L	sound pressure level
m	Meter
m	mass
MB	Minas Basin
MC	Minas Channel
MP	Minas Passage
ms	Millisecond
m/s	Meters per second
MW	Mega-watt
n_i	number of clicks within a bin
N	Sample size
Na	Not applicable
NBHF	Narrow Beam High Frequency

NOAA	National Oceanic and Atmospheric Administration
p	pressure
$p(x)$	proportion of x
Pa	Pascal
PAM	Passive Acoustic Monitoring
PPS	Pulse Per Second
PTS	Permanent Threshold Shift
r^2	radial distance
re or ref	Reference to
RHIB	Rigid Hull Inflatable Boat
s	signed current speed
S	salinity
SARA	Species At Risk Act
SE	Standard Error
sec or s	Second
SD card	Secure Digital card
SUB	Streamlined Subsurface Buoy
t	time
T	wave period
T	Temperature in °C
TISEC	Tidal In-Stream Energy Conversion
TTS	Temporary Threshold Shift
u	velocity
UTC	Coordinated Universal Time
V	Vertical
w_i	size of bin
WADPM	Windowed Acoustic Detection Positive Minute
WVDPM	Windowed Visual Detection Positive Minute
z	depth
3D	Three-dimensional
µs	Microsecond
µPa	Micro-Pascal
α	seawater absorption coefficient for sound energy
@	at
°	Degree (angle)
°C	Degree Celsius
Δ	Delta
ρ	density
%	Percent
π	pi

ABSTRACT

The environmental effects monitoring program for tidal energy development at the Fundy Ocean Research Center for Energy test facility in Minas Passage requires examination of the effects on marine life, and includes Atlantic harbour porpoise, *Phocoena phocoena* (Linnaeus, 1758). All prior passive acoustic studies of porpoises in Minas Passage have used stationary, bottom-moored acoustic recorders (CPODs and icListenHF). Flow noise and noise associated with moorings and mobile sediments were identified as major issues for the acoustic detection of porpoises. The present study employed a custom designed drifting hydrophone (icListenHF) array to mitigate the effects of flow noise and moorings on passive acoustic harbour porpoise monitoring. The drifting array was deployed for a 5-7 hour drift on each of six days during 12th - 27th June 2017. Harbour porpoise presence and behaviour, detected using the newly developed Coda click detector, was assessed in Minas Passage and adjacent areas. The effects of short-duration anthropogenic noise from fishing vessels and other boat traffic were found to have no observable effect on porpoise presence. The multi-hydrophone array detected porpoise clicks generated both above and below 15 m. Spatio-temporal and current speed patterns in porpoise activity were observed, with porpoise activity being lowest in Minas Basin, during early afternoon (1500-1700 UTC), and when current speed was <1 m/s. The Coda detector was effective in identifying three behavioural modes in the harbour porpoise inter-click interval data. These were classified as feeding, searching and navigation trains. A novel finding was patterned clusters of clicks in most feeding trains and in 25% of search trains. This study will serve to inform future use of drifting hydrophone arrays for assessing harbour porpoise presence, abundance and behaviour in Minas Passage and, potentially, at high flow sites elsewhere.

1.0 INTRODUCTION

1.1 Sound and Marine Mammals

Various marine organisms, including Cetaceans (whales), have evolved characteristics and behaviors to both generate and utilize sound in their environment. Mysticetes (baleen whales) use sound primarily for communication, display and to establish territory (Richardson *et al.* 1995; Bannister 2009). Odontocetes (toothed whales, including dolphins and porpoises) use sound as a means of communication, but also rely on echolocation to navigate, forage and interact with their environment (Au 1999; Richardson *et al.* 1995). The ability of whales to communicate and echolocate, however, may be modified by anthropogenic changes to the ambient marine soundscape (Tyack 2008).

This thesis focuses on the Atlantic harbour porpoise, *Phocoena phocoena* (Linnaeus 1978), and the use of passive acoustic monitoring technologies, a drifting platform, and newly developed porpoise click detection software to monitor porpoise echolocation activity. The study was conducted in Minas Passage and adjacent high current speed environments where tidal energy development is underway. The following sections describe background material related to the measurement of marine sound and the detection of echolocation vocalizations of the Atlantic harbour porpoise.

Sound is a pressure wave with a pattern of compressions and rarefactions which propagate in water at about speed c = 1500 m/s. Sound is measured by two metrics: intensity and frequency. Sound intensity is measured in units of pressure and can be represented linearly using Pascal (Pa) or logarithmically using decibels (dB). The intensity of sound in water declines as it propagates due to attenuation and radial

spreading. An observer at a fixed point will see the sound wave pass at speed *c*. Thus, the observer will see a complete oscillation in a time $T = l/c$ [s]. This time is called the wave period. The frequency at which a wave passes is the reciprocal of wave period and is given the symbol *f* and units of Hz [1/s]. Appendix I provides a more detailed overview of the dynamics of sound in water.

1.2 Natural Sound Sources

A major factor that dictates natural ambient noise is sea state, with ambient noise rising with increased wind and wave action, and rainfall (Richardson 1995). In high flow sites, waves can become steep when the tide flows against the wind and may thus increase sound level. Where current is fast, as in Minas Passage, contributions to ambient noise also include mobilized bottom sediments (Fader 2009). Noise caused by sediments is usually in the frequency range 1–30 kHz, although small particles can create higher frequency noise (max. 400 kHz) (Thorne 1986).

Increased sound levels associated with weather (wind and rain) and tidal current are relatively long duration events which contribute to the mid-frequency band (500 Hz to 25 kHz) of the sound-scape (Hildebrand 2009). Natural events that cause short duration changes to the sound-scape of an aquatic environment are low frequency seismic waves (earthquakes) and bio-acoustic sound generation (e.g. marine mammal echolocation, shrimp clicking) (Hildebrand 2009). In Minas Passage, ambient sound level is mostly associated with the tidal current (Sanderson *et al.* 2017).

1.3 Anthropogenic Sound Sources

Anthropogenic noise in marine environments has increased exponentially in the recent past as shipping traffic, industrial developments and seismic testing have

become more prevalent (Hildebrand 2009). These noise sources have led to an increase in the overall ambient noise in the ocean as well as an increase in peak noise level (Hildebrand 2009). Anthropogenic noise in the ocean is classified by two descriptors: intensity and duration. These classifications enable anthropogenic sound to be classed as acute or chronic.

Acute anthropogenic noise is short duration with an intensity over 150 dB. Some examples of acute anthropogenic noise are marine construction activities and military exercises (Tyack 2008). Construction activities, like seismic air gun surveys and pile driving used in the installation of marine renewables and oil rigs, can generate high intensity sound (180 dB re 1µPa) (Tyack 2008). Military activities, including the use of high powered sonar and explosives, are additional sources of acute anthropogenic noise (Hildebrand 2009, Table 1).

Chronic anthropogenic noise is long duration, with average peak intensity less than 150 dB. The largest contributor to chronic noise in ocean waters is shipping noise, which is created by the vessel's propulsion system (Tyack 2008). Cavitation caused by propeller blades generates broadband noise and tonal components (Hildebrand 2009, Table 1). Much of the acoustic energy created by shipping is situated in frequencies bands < 200 Hz (Hildebrand 2009). In the present hydrophone study, vessel noise was largely from fishing vessels but with noise detected over short periods of time.

1.4 Effects of Anthropogenic Marine Sound on Marine Mammals

Anthropogenic sound increases the ambient noise levels experienced by marine mammals, and thus changes the sound niche. Baleen whales, or Mysticeti, use low frequency calls to communicate over long distances with others of the same

species. These calls communicate distress, identity, stress, reproductive status, and presence of food resources (Richardson *et al.* 1995). Toothed whales, or Odontoceti, communicate similarly with sound. Additionally, odontocetes use biosonar to navigate, inspect objects, and locate prey in their environment (Richardson *et al.* 1995).

With increasing anthropogenic activities in the ocean environment, the total ambient noise levels are rising. Consequently, marine animals that use the sound niche have to adapt to louder conditions. Negative effects of increasing noise levels on marine mammals manifest in two forms: physiological and behavioral.

1.4.1 Physiological

The main physiological effects of an increase in anthropogenic noise are hearing damage and increased stress (Weilgart 2007). Hearing damage can occur in two ways: a temporary threshold shift (TTS) and/or a permanent threshold shift (PTS). Marine mammals exposed to a sound that has high intensity and/or long duration can experience temporary changes to their hearing, which can occur across a wide or narrow frequency band (Weilgart 2007). PTS can occur if the sound is at a high intensity and for a long enough duration that the acoustic pressure irreparably damages one or more of the hearing organs (e.g. ruptured eardrum) (Weilgart 2007).

Exposure to anthropogenic noise can also induce physiological stress responses in marine mammals. Romano *et al.* (2004) showed that beluga whales, *Delphinapterus leucas* (Pallas 1776) and bottlenose dolphins, *Tursiops truncatus* (Montagu 1821), experienced raised levels of hormones related to stress when exposed to high intensity anthropogenic sound (e.g. air gun).

1.4.2 Behavioural

In addition to the physiological effects of anthropogenic noise, marine mammals can undergo behavioral changes in response to raised ambient noise levels. Changes in vocalizations, avoidance behaviour, and shore strandings are all common responses to increased anthropogenic noise (Nowacek *et al.* 2007).

Effects on vocalization that have been observed in response to anthropogenic noise include changes (increase or decrease) in number, intensity and frequency of vocalizations (Lesage *et al.* 1999; Foote *et al.* 2004; Buckstaff 2004; Scheifele *et al.* 2005). The Lombardi vocal response, which is vocalization level increasing in direct response to increased ambient noise, has been observed in beluga whales in the St. Lawrence River (Scheifele *et al.* 2005).

Marine mammal avoidance of areas with high levels of anthropogenic noise can have catastrophic effects at the population level (Weilgart 2007). Access to areas that are important feeding grounds, migratory routes or breeding areas could be altered by anthropogenic activity and related noise levels (Weilgart 2007). Industrial noise virtually excluded Grey whales from their San Ignacio breeding lagoon for more than 5 years (Jones *et al.* 1994). Other studies have concluded that harbour porpoise do not undergo broad-scale, long-term displacement when exposed to increases in anthropogenic noise (pile-driving) (Brandt *et al.* 2011; Thompson *et al.* 2013). However, porpoises may experience both small-scale, short-term displacement and increases in echolocation activity when exposed to anthropogenic noise (e.g. 2 MW wind turbine) (Koschinski *et al.* 2003).

Increases in strandings have also been linked to anthropogenic noise, where increased stress and injuries caused by noise result in marine mammals beaching

themselves at a higher than normal rate (Weilgart 2007). In 2009, Naval exercises involving military-grade sonar near the Bahamas resulted in a multi-species mass stranding and deaths of Cuvier's beaked whales, Blainville's beaked whales, Minke whales, and a spotted dolphin (Evans *et al.* 2001).

1.5 Harbour Porpoise

This study examines the presence and behaviour of Atlantic harbour porpoise (*Phocoena phocoena)* in a high flow tidal energy development site in Minas Passage, Bay of Fundy. This small-sized, coastal marine mammal species is vulnerable to human activities, especially fishing, and is thus currently designated as a species of 'Special Concern' by the Committee on the Status of Endangered Wildlife in Canada (COSEWIC). Atlantic harbour porpoise is listed as 'Threatened (Schedule 2)' under the Species at Risk Act (SARA) and is also protected from disturbance in Canadian waters by Marine Mammal Regulations (2017).

1.5.1 Biology and Ecology

Harbour porpoise typically reside in temperate and boreal waters that are less than 200 metres in depth (Bjørge and Tolley 2009). Within Canada, Atlantic harbour porpoises are divided into three subpopulations: Newfoundland-Labrador, Gulf of St. Lawrence, and Bay of Fundy-Gulf of Maine (Gaskin 1984,1992). The sub-population of interest for this study is the Bay of Fundy-Gulf of Maine sub-population. Harbour porpoise activity in Minas Passage peaks in spring and fall (Wood *et al.* 2013; Porskamp *et al.* 2015), mirroring the timing of movements of migratory fish species (many of which are porpoise prey) between Minas Basin and Minas Channel and beyond (Dadswell, 2010).

Atlantic harbour porpoise females have an average length of 160 cm and weigh an average of 60 kg; males are smaller having a length averaging 145 cm and weighing an average of 50 kg (Bjørge and Tolley 2009). Harbour porpoises have a short, rounded snout and a short triangular dorsal fin with a broad base (Figure 1) (Balcomb *et al*. 1983). They have a typical life-span of 8-10 years (observed maximum age of 23 years), with females birthing one calf per year after age 3 (Bjørge and Tolley 2009). Females carry the fetus for a gestation period of ~10.5 months and calves are weaned at approximately one year (Bjørge and Tolley 2009). Harbour porpoise travel alone, in small groups, or in a mother-calf pairing (COSEWIC 2006).

In the Bay of Fundy, Atlantic harbour porpoise prey mostly on Atlantic herring, *Clupea harengus* (Linnaeus 1978) and alosine herring, *Alosa pseudoharengus* (Wilson 1811) (Recchia and Read 1988). When herring are unavailable, the prey intake is supplemented with juvenile gadids and small groundfish (Recchia and Read 1988). Calves transition from milk to solid food by feeding on euphausiids while learning to hunt for larger fish species (Smith and Read 1992). In the Bay of Fundy, harbour porpoises are considered top-tier predators due to the rarity of their natural predators, transient killer whales, *Orcinus orca* (Linnaeus 1758), and large sharks (COSEWIC 2006; 2008).

The largest threat to the Bay of Fundy harbour porpoise population is bycatch in fishing gear. However, the severity of this threat has decreased with shrinking groundfish stocks and an associated decrease in fishing effort (COSEWIC 2006).

1.5.2 Echolocation

Harbour porpoise use echolocation for navigation, and for locating and capturing prey (Villadsgaard *et al.* 2007). Porpoises produce vocalizations called

clicks by passing air between air sacs, through phonic lips, located in their nasal passages. The clicks are given directionality and focus (~15° beam) using the fatty melon at the head of the animal (Verfuß *et al.* 2009; Au 1999; Goodson and Sturtivant 1996) (Figure 1). Once the click has interacted with an acoustically reflective object (e.g. prey), the return signal is received by a fatty deposit surrounding the porpoise's lower jaw. The signal is transferred to the inner ear, then to the brain (Verfuß *et al.* 2009).

The audiogram of a harbour porpoise ranges from 0.25 – 180 kHz and is most sensitive at frequencies from 100 -140 kHz (Figure 2) at a sound level threshold of 35 dB (Kastelein *et al.* 2002). Interestingly, one of the porpoises' main prey species, alosine herring (gaspereau and shad), have a similar audiogram range (~0.25 – 180 kHz) (Figure 2). Alosine herring possess less sensitive hearing, therefore require higher sound levels to hear high frequencies (Mann and Popper 1997). This shows that alosine herring can detect harbour porpoise echolocation clicks, albeit at a short distance (10s of meters), based on their audiogram (Figure 2) and modelled attenuation of porpoise click sound level (See Appendix, Figure A2).

Harbour porpoise echolocation clicks are short in duration, ranging from 75 – 150 µs (Villadsgaard *et al.* 2007). They have a frequency of ~130 kHz and a maximum source level of 172 dB re 1 µPa @ 1 m (Villadsgaard *et al.* 2007). A sequence of clicks, generated by the same animal over a relatively short interval, is a click train. The echolocation clicks in a harbour porpoise click train do not vary significantly in frequency but do have a variable inter-click interval (ICI) (Verfuß *et al.* 2009).

Variable ICI is exhibited by the harbour porpoise in different phases of prey capture (Verfuß *et al.* 2009). The maximum ICI of harbour porpoise is 250 ms, and consecutive clicks within 250 ms are classified as a single click train (Villadsgaard *et al.* 2007). Harbour porpoise echolocation ICI patterns are associated with behaviors such as search and approach (to prey), with the approach phase further divided into initial and terminal buzz/feeding buzz phases (Verfuß *et al.* 2009), similar to the echolocation phases observed in insectivorous bats (Griffin *et* al 1960; Melcón *et al.* 2007). Verfuß *et al.* (2009) identified a prey search phase with an ICI range of 30 – 100 ms, with the approach phase beginning at 30 ms and dropping to 1.5 ms immediately prior to prey capture.

1.6 Measuring Marine Sound

Sound is detected by animals when the pressure waves cause vibrations in the auditory system. The pressure compressions and rarefactions caused by acoustic waves can also be measured using hydrophones.

1.6.1 Hydrophones, Data Processing and Signal Detection

Hydrophones detect minute changes in pressure measured in micro-Pascals through a piezoelectric transducer situated in the listening element (Li *et al.* 2002). The piezoelectric transducer generates electricity when subjected to pressure changes (Li *et al.* 2002). The electric signal is fed through a series of pre-amplifiers, filters, and analog/digital converters before finally being stored in a digital format that can be viewed on a computer (Ocean Sonics 2012). Three common ways to visualize acoustic data are time-series (waveform), spectrum, and spectrogram.

Time-series (waveform) data consists of N measurements of pressure p at a sampling interval Δ. Thus, the discrete times t at which measurements are made can

be written $t_k = k\,\Delta$ where $k = 0, 1, 2, 3, \ldots, N\text{-}1$. At these times the discrete pressure p measurements are $p_k = p(t_k)$. A time-series plot is simply the values of p_k plotted against the values of t_k. Figure 3 is a time-series plot used to highlight a harbour porpoise click train, which can be seen in greater detail in Figure 3b. Figure 3c highlights a singular harbour porpoise click within the click train. Clicks similar to this can be used as a template in automated click detection.

In order to understand the spectrum and spectrogram we need to introduce the Discrete Fourier Transform (DFT). The DFT is another way to exactly represent the measurements of p_k as the sum of sine and cosine functions that oscillate at discrete frequencies $f_n = n/(N\Delta)$, where $n = -N/2, \ldots, N/2$ and N is an even number. We represent the amplitude of oscillations at frequency f_n by A_n for cosine part, and B_n for sine part in the following DFT

$$A_n = \sum_{k=0}^{N-1} p_k \cos(2\pi kn/N) \qquad \text{(Eq. 3)}$$

$$B_n = \sum_{k=0}^{N-1} p_k \sin(2\pi kn/N) \qquad \text{(Eq. 4)}$$

The original time-series p_k can be reconstructed from the amplitudes (A_n and B_n) of the frequency components f_n as follows

$$p_k = \frac{1}{N}\sum_{-N/2}^{N/2}[A_n \cos(2\pi kn/N) + B_n \sin(2\pi kn/N)] \qquad \text{(Eq. 5)}$$

Thus, the p_k represents the acoustic signal in the time domain t_k and the discrete Fourier components A_n and B_n represent the same signal in the frequency domain f_n. From Equation 5 it is clear that the DFT contains all the information in the original time-series and vice-versa.

There are many advantages to considering the DFT as well as the original time-series. The DFT enables us to see the extent to which different frequencies of

oscillation determine the original time-series. This is called spectral analysis. Porpoise clicks have short duration and can be very difficult to find in a time-series plot. However, if we look at the power $A_n^2 + B_n^2$ of high frequency Fourier components plotted against f_n (the spectrum), then the presence of porpoise clicks can become much more apparent.

The DFT also provides us a means of filtering the time-series p_k with respect to frequency f_n. Setting the Fourier components A_n and B_n to zero for high frequencies enables us to calculate a low frequency time-series using Equation 5. Low frequency information in the time-series can be preserved even if Δ is made much larger. Thus, the low frequency information can be preserved with much less storage space.

Setting the Fourier components A_n and B_n to zero for low frequencies enables us to view high frequency information (porpoise clicks) without it being obstructed by low frequency information. Since porpoise clicks are high frequency they can be seen in the Fourier Transform of relatively short time series. Thus, when looking for porpoise clicks, we can divide a long time-series p_k into many consecutive, short periods. Obtaining the spectrum for each short period and plotting successive spectrums side by side gives us the spectrogram. Thus, the spectrogram is typically plotted with time increasing along the horizontal axis, frequency on the vertical axis, and a colour scale to represent the amplitude of frequency components at each time (Audacity 2017). Times at which porpoise clicks are present appear as high amplitudes at the frequencies used by porpoises (Figure 4).

Automation of the signal detection process is important when dealing with large quantities of acoustic data. The optimal technique for finding a known signal (e.g. porpoise click) in a time series of acoustic data is a matched filter (Zimmer

2011). Matched filters are commonly used in radar and sonar technologies, where it is necessary to distinguish the generated radar/sonar signal against the background noise. Essentially a matched filter multiplies a template signal by the raw signal. Portions of the signal that match the template will create a multiplicative spike in the time-series while portions that do not match will be cancelled out or suppressed. Therefore, a matched filter increases the signal to noise ratio of the data. Setting a signal energy threshold (dB or Pa) across the data set allows for filtering out all but the signal that matched the template (Zimmer 2011).

Matched filters can be used in conjunction with a correlation function to assess the correlation between the template signal and the signal identified by the matched filter. Using this approach, the Coda porpoise click detector was recently developed (Sanderson, unpublished) for use with the icListenHF (Ocean Sonics Ltd.) hydrophone and was adopted for the present study. The Coda software program uses a matched filter to automate the detection of harbour porpoise clicks within an acoustic file. Additionally, the program's output can be interactively reviewed with post-processing software that uses spectrograms, various correlation functions, and signal context in order to assess the quality of the detected clicks. Currently, work is being done to integrate the Coda click detector into the onboard software of the icListenHF hydrophone.

1.6.2 Passive Acoustic Monitoring: Marine Mammals

Hydrophones are passive acoustic monitoring (PAM) instruments used to collect acoustic recordings, including sounds produced by animals (Zimmer 2011). The hydrophones can be attached to stationary platforms, housed within tethered moorings (sub-buoys) or attached to a drifter. The advantages and disadvantages of each method of deployment are described in Table 2.

The recordings are analyzed for unique acoustic signatures produced by the study species in question. PAM is now commonly used in marine mammal surveys and research to replace or augment visual surveys which are logistically complex, labor intensive, and restricted to operating in the daylight hours under pristine weather conditions. Visual surveys are impeded by darkness, rough seas, rain, and fog. Gulf of Maine/ Bay of Fundy harbour porpoise visual surveys in 1991 and 1992 noted that data collected during Beaufort Sea state greater than 2 could be negatively biased (Palka 1996).

1.6.3 Effects of Flow on Acoustic Measurements

The use of acoustic instrumentation for monitoring in marine environments becomes increasingly difficult as current speed increases (Table 2). Water flowing at high speeds past the hydrophone creates flow noise, which results from local random pressure fluctuations caused by turbulence being detected by the hydrophone element (Strasberg 1985). Both noise from mobilized sediment and flow noise have the potential to mask acoustic signals of interest (Sanderson *et al.* 2017*).*

1.7 Use of Hydrophones for Detecting Porpoise Presence and Behaviour

Prior PAM studies in the high flow environment of Minas Passage have been used to assess trends in porpoise activity at the FORCE test site, using a combination of automated click loggers (CPODs) (Tollit *et al.* 2011; Wood *et al.* 2013) and high frequency hydrophones (icListenHF) (Porskamp *et al.* 2015). These studies used detection positive minutes (DPM, minutes with at least one porpoise click detection) as an activity indicator, with an increase in DPM signifying an increase in porpoise presence.

Porpoise inter-click intervals (ICI) provide higher resolution information than DPMs and relates to behaviour such as foraging and feeding activity (Koschinski *et al*. 2008). A sudden drop in porpoise ICI below 10 ms to as low as 1.5 ms indicates a terminal or feeding buzz, which occurs close to and immediately before prey capture (Koschinski *et al* 2008).

A synchronized array of hydrophones deployed at a site or on a drifter offers the ability to collect massive amounts of acoustic information that can be verified against other hydrophones in the array. The acoustic array can also be used to localize a sound source. Using the difference in time that two or more hydrophones record the same signal, such as an echolocation click, information pertaining to a position of origin can be calculated. Obtaining the click source location is useful for calculating the number of animals being detected and a necessary step for estimating porpoise abundance.

1.8 FORCE Tidal Energy Test Site and Sound Source

Turbine demonstrations at the FORCE test site in Minas Passage will increase environmental noise levels due to installation and recovery activities, increased boat traffic, operational noise from the tidal instream energy conversion (TISEC) devices, and signals emitted from active acoustic sensors on the turbine infrastructure and nearby stationary monitoring platforms. How these various sound sources contribute to the ambient soundscape is poorly known, although there have been recent attempts to investigate the overall effect of a Cape Sharp Tidal – Open Hydro turbine on ambient noise levels (Martin and Horwich 2018).

1.9 Objectives

Tidal energy developments in Minas Passage and adjacent areas are regulated and require environmental effects monitoring programs. Given the high current speeds in Minas Passage and flow issues associated with stationary hydrophones, drifting hydrophone arrays may serve to provide higher quality data on the soundscape, and both presence and behaviour of Odontocetes. Additionally, an array of hydrophones can be used to assess the vertical distribution of harbour porpoise in the water column, in relation to the depths spanned by turbines planned for installation.

The aim of this project is to address information and technology gaps related to the assessment of harbour porpoise activities in Minas Passage and adjacent areas. The objectives are to:

1. Design and construct a multi-hydrophone drifter to minimize both flow noise and noise associated with surface waves;

2. Examine trends (temporal, spatial and tidal) in harbour porpoise presence and activity, using data collected with a drifting hydrophone array;

3. Determine depth distribution of harbour porpoises via detection of clicks generated above and below the vertical mid-point (15 m) of two hydrophones. The limitations of using an array of only two hydrophones are also explored.

4. Examine the relationship between harbour porpoise click train detections and A) visual observations of a harbour porpoise, and B) presence of anthropogenic noise sources (e.g. fishing vessels and turbine testing operations);

5. Examine patterns in the inter-click intervals of porpoise click trains for evidence of behavior (e.g. feeding).

2.0 METHODS

2.1 Study Site Description

The Inner Bay of Fundy is a semi-diurnal, hyper-tidal system with a tidal range of 11-17 m and surface current speeds up to 6 m/s (Karsten *et al.* 2008). The 5.5 km wide and 14 km long Minas Passage connects Minas Channel to Minas Basin. The maximum depth within Minas Passage is approximately 170 m (Figure 5) (Fader 2009).

Minas Passage is an important migratory route for economically important species, including alewife *Alosa pseudoharengus* (Wilson 1815), American shad *Alosa sapidissima* (Wilson 1811), Atlantic herring, Atlantic mackerel *Scomber scombrus* (Linnaeus 1758), and striped bass *Morone saxatilis* (Walbaum 1792) (Dadswell 2010). Protected species that utilize Minas Passage as a migratory route include Atlantic salmon *Salmo salar* (Linnaeus 1758), American eel *Anguilla rostrata* (Lesueur 1821) and Atlantic sturgeon *Acipenser oxyrinchus* (Mitchill 1815) (Dadswell 2010).

Minas Passage is also home to the Fundy Ocean Research Center for Energy (FORCE), a facility developed for testing new Tidal In-Stream Energy Conversion (TISEC) technologies. During our field studies, a 16 m diameter Open Hydro tidal turbine (Figure 6a), which had been operational since its deployment in November 2016, was recovered with the aid of several tug boats and a barge (Figure 6b). The turbine was successfully retrieved on the 15th June 2017 while our drifter was moving through Minas Channel.

2.2 Drifter Design and Instrumentation

The drifter consisted of a high visibility pole float equipped with a GPS logger (Garmin GPSmap 62s) tethered to a subsurface unit with a set of three 20 cm spherical floats and a lead weight (~11.5 kg) (Figure 7). Various acoustic sensors were mounted at 1-2 m intervals on the 12 m section of rope between the flotation units and the weight. Total length of the drifter was approximately 20 m. Equipment load-out consisted of two synchronized icListenHF hydrophones, two Chelonia CPODs to log detections of porpoise clicks, and two Vemco VR2Ws (69 kHz) which were included for the opportunistic detection of acoustically tagged fish. On five of six drifts, a waterproof action camera (GoPro Hero3 White Edition) was mounted above the flotation unit, 6-7 m below the surface, to observe harbour porpoise should they come close to the drifter.

2.2.1 IcListenHF Hydrophone

The icListenHF is a high frequency (512000 samples/second) smart hydrophone developed and manufactured by the Nova Scotia based Ocean Sonics Ltd. hydrophone company (Figure 7). A "smart" hydrophone incorporates parts of the signal processing into an internal computing board. The computing board, along with internal battery and data storage allows the icListenHF to be deployed as an autonomous unit. Recording parameters like duty cycle, and sampling rate/ frequency were set prior to deployment.

An on-board computer allows multiple icListenHFs to be synchronized using a synchronization cable. Synchronization requires one hydrophone to be set as the "master" and one to be set as the "slave". A pulse-per-second or PPS is sent from the master hydrophone through the synchronization cable to the slave hydrophone. The

slave decodes the time from the PPS. The hydrophones used in this study were synced to +/- 122 nanoseconds (Ocean Sonics Ltd, pers comm, 2017).

2.2.2 CPOD

The CPOD (Chelonia Porpoise Detector) is an autonomous passive acoustic click logger developed by Chelonia Ltd (Figure 7). CPODs record the detection of high frequency click trains produced by harbour porpoises and other Odontocetes. Although they serve as a hydrophone, the CPODs do not store time series data but rather log click trains by saving details like sound pressure amplitudes, frequencies, and click envelope in order to minimize data storage space. CPODs are designed for long deployment times, with battery (8 alkaline D-cells) and data storage (4 GB SD card) capable of about 4 months of continuous recording.

CPODs have been deployed extensively in and near the FORCE CLA since 2010 and contribute to the ongoing environmental effects monitoring program. Compared to the icListenHF hydrophone technology, CPODs have a shorter detection range (100-300 m) and can have performance issues in noisy, high current sites (Wood *et al.* 2013, Porskamp, 2015). Because CPODs continue to be used with SUBs moorings at multiple sites in/near FORCE, they are included in this drift study to allow a comparison of their effectiveness at detecting harbour porpoise echolocation click trains while in drifting mode.

2.3 Drifter Deployment and Retrieval

Six drifts (three ebb/three flood) were conducted in Minas Passage and adjacent areas during June 12th, 14th, 15th, 16th, 26th and 27th, 2017. Due to the tidal cycle being lagged from one day to the next, and inclement weather conditions, it was not possible to complete all drifts on six consecutive days. Four of the six drifts were

completed in the first five days (3 flood/1 ebb), on or near a neap tide. The remaining two drifts (ebb tide) were completed near the following spring tide.

Assembly of the drifter was conducted prior to each deployment. The two icListenHF hydrophones were activated and attached together via synchronization cable during the later stages of drifter assembly. Once connected, the icListenHFs were synced within 2 minutes.

The CPODs were activated the day before the day of deployments, then soaked in water until deployment (~24 hours) for full wetting of the transducer housing, which allows for full sensitivity. Since CPOD battery capacity allows for continuous operation over several months, the CPODs were operational for the duration of the study.

Two Vemco VR2W units, which allowed opportunistic detection of acoustic fish tags, were mounted above and below the CPODs. These units were activated the day before the first round of deployments and, like CPODs, were active for the duration of the study.

When on site, the drifter was manually deployed from the side of a small (5.5 m) Rigid Hull Inflatable Boat (RHIB). The RHIB was captained by Randy Corcoran and was launched from the western facing rock beach of the isthmus of Partridge Island. This launch site permitted the boat to be launched at almost any phase of the tide. The field crew consisted of myself (Mike Adams) and Dr. Brian Sanderson. The vessel was equipped with an echo-sounder operating at approximately 117 kHz, which remained off for nearly the entire time that the drifter was deployed. Records of echo-sounder status (on/off) were maintained in the field log book.

Once the drifter was deployed the RHIB operator shut down the engines and drifted within 800 m of the drifter until it was retrieved. Drift duration was 5 -7 hours long and varied depending on the light conditions and the tidal cycle. As visual contact needed to be maintained to retrieve the drifter at the end of each deployment, the drifts were conducted only during daylight. Drifter retrieval was accomplished by positioning the RHIB alongside the drifter and manually removing it from the water.

Two Garmin GPSmap 62s handheld devices were used to automatically log the position of the drifter and the position of the boat, at 5 second intervals with an accuracy of ± 5 m (Garmin Ltd 2011). One GPS logger was mounted on the surface pole float (Figure 7). The other GPS logger remained on the boat and was kept on deck to ensure strong satellite reception. Depending on the start location and trajectory of the drifter, the drift track was sometimes extended into Minas Basin or past Cape Spencer (Figure 5).

Visual observations were made by the field crew throughout the duration of all the drifts. Harbour porpoise sightings were recorded in the field log book, noting time, number of individuals, bearing and an approximate distance from the RHIB. Sources of anthropogenic noise (RHIB movements, fishing vessels, tidal turbine recovery operations, and airplanes) and the time of their occurrence were also recorded in the field log book.

2.3.1 Weather Consideration

Due to safety concerns and weather-related risk of losing equipment, the drifts were conducted primarily on days when the predicted wind speed was less than 15 knots. The weather ranged from clear skies to moderate rainfall. Inclement weather such as rain, cloud cover, and wind reduced our effective line of sight. Additionally,

high wind often displaced the RHIB. While a sea anchor was used to reduce boat drift, it was necessary to reposition the RHIB more frequently on windy days than during drifts completed on calm, low wind days.

2.4 Data Processing

IcListenHF acoustic data was downloaded within hours after each completed drift. The data was transferred from the hydrophone to an external drive using Filezilla file transfer system (Filezilla 2017). The data stored in the GPS loggers were downloaded using Garmin Basecamp and exported into a *.txt* file, then stored on an external drive. CPOD data was downloaded from the SD cards to an external drive following completion of the study.

The majority of the icListenHF data analysis was completed using programs created and run in MATLAB (MATLAB and Statistics Toolbox 2016). Programs were also created and run using the C programming language to take advantage of their greater computation speed.

The Coda software, a C program developed by Brian Sanderson in partnership with Ocean Sonics Ltd, was used to detect harbour porpoise clicks. A broad band filter (100 – 150 kHz) is applied to the raw acoustic data (.wav files). Coda then uses a matched filter using a theoretical porpoise click generated from prior studies.

When a click is located, the energy (Pa^2) in the frequency band used by porpoises (124 – 138 kHz) is compared to the energy in the neighbouring bands. If the energy of the neighbouring bands is high relative to the energy in the porpoise band the click is discarded. The resulting data is then run through a MATLAB program (*calc_pdm.m*) that filters out the clicks that have a sound level less than 110 dB and signal to noise ratio less than 2.5. *Calc_pdm.m* is also responsible for grouping the

clicks into click trains. *Dlg_review_trains.m*, a third MATLAB program, is used to manually review and fill gaps created in click trains by the stringent filters used in the programs above. Clicks are added when a click train has obvious missing clicks between detections. One click is added to the start and end if it is apparent in the spectrogram. Clicks are apparent in the spectrogram when they are observed as a narrow band high frequency click of the correct duration (~150µs) and frequency range (124 – 138 kHz) for a harbour porpoise vocalization. The Coda software cannot always distinguish individual clicks within a feeding buzz, therefore a separate program, *Madd_buzz.m,* is used to manually add clicks by visually inspecting the matched filter convolution plot. The files containing the manually added clicks are used to increase the accuracy of the ICI analysis. The binning of the data in DPM was achieved using multiple MATLAB scripts.

The CPOD data was processed using the Chelonia CPOD.exe program. The click logger's data file (CP1 file) is read into the CPOD.exe program, where the click trains are filtered to remove chance trains from non-marine mammal sources (rain, crustaceans, and mobilized sediment particles). A quality value of either High, Moderate or Low is assigned. Due to the high false-positive rate of the Low quality click trains, only Moderate and High-quality trains were included for further analysis. Secondarily, the clicks are classified by type of click, which is determined by an assessment of the inter-click interval (ICI), frequency, and length/amplitude of the click trains. Narrow Band High Frequency (NBHF) trains are classified as harbour porpoise click trains. The resulting file (CP3 file) is then exported in terms of DPM (Detection Positive Minutes).

The Garmin GPS data was downloaded into Garmin Basecamp (Garmin Ltd 2016) then exported in plain-text files. The GPS text files were imported into

MATLAB for use in the spatial analysis of the click detections, drifter position and current speed.

2.5 Data Analysis

2.5.1 Drifter Tracks

The drifter tracks were mapped onto a bathymetric map of Minas Passage and adjacent areas (Figure 5). The tracks were trimmed at the start and end to omit periods of drifter deployment and recovery noise.

2.5.2 Passive Acoustic Detections

The question arose as to whether or not the two hydrophones (icListenHF 1211 and 1239) detected porpoise clicks with equal effectiveness. Synchronization allowed harbour porpoise click detection performance of the two hydrophones to be compared against one another. The comparison of the units was not entirely trivial to address, as the hydrophones were deployed at different vertical positions (14 m and 16 m) on the array depending on the drift. For the first two days, icListenHF 1211 was in the upper position and for the last four days icListenHF 1239 was in the upper position. The number of clicks detected by each hydrophone was calculated, as described above, for each of the 1903 minutes sampled over the six study days. The program *cf_instruments_top_bottom.m* was written to make the comparison analysis shown in Table 3.

Comparing visual sightings of porpoises with hydrophone acoustic detections is made difficult by the many differences between these two methods of observation. Acoustic detections only happen when a porpoise is sufficiently close to the hydrophone and oriented so that the hydrophone is within the 15° beam width of the porpoise click. Because clicks with a sound level less than 110 dB were excluded

from the analysis, the maximum range for a porpoise click detection was about 300 m (Appendix, Figure A2). Human observers, on the other hand, can scan a wide field of view and on a good day may see a surfacing porpoise at ranges well beyond 300 m. However, a porpoise surfaces only briefly. Also, the hydrophone compiles a nearly continuous record whereas visual sightings were not continuously documented, although more effort should be made in this regard in the future.

In order to compare DPM with visual observations, a windowing operator is required. This is because a porpoise is unlikely to have its clicks acoustically detected at the time it is visually observed. It is more likely to be acoustically detected within minutes before or after a visual sighting.

The program *cf_visual_acoustic.m* was written to compare visual and acoustic detections. The algorithm begins by documenting each of the 1903 minutes measured as either detection positive or detection negative, thus giving two sequences of true/false values, one for acoustic detections and one for visual detections. A 10-minute window was then run over each sequence so that a minute would be true if any of the minutes ± five minutes recorded a click (for the acoustic sequence) and a sighting (for the visual sequence).

In this study, the windowed sequences were called WADPM (windowed acoustic detection positive minutes) and WVDPM (windowed visual detection positive minutes. Two fundamental questions were asked:

1) Are acoustic detections more likely when there are visual detections than when there are not visual detections?

2) Are visual detections more likely when there are acoustic detections than when there are not acoustic detections?

Both of these questions can be addressed by considering proportions of time that are detection positive under some condition. Thus, we write *p*(WADPM | WVDPM) to mean the proportion of the WADPM sequence that is true, subject to the condition that WVDPM is true. Effectively, we select those elements of WADPM that correspond to WVDPM being true and then calculate the proportion of that selection that is true. The usual rules for categorical date are used to compute a standard error for the proportion. The proportion *p*(WADPM | WVDPM) is a measure of when the acoustic method detects a porpoise subject to the visual method detecting a porpoise.

Similarly, we write *p*(WADPM | NOT WVDPM) to mean the proportion of the WADPM sequence that is true subject to the condition that WVDPM is false. Thus, this proportion is a measure of when the acoustic method detects a porpoise subject to the visual method not detecting a porpoise. The analysis can be reversed, to obtain the proportions when the visual method detects a porpoise, subject to the acoustic method either detecting a porpoise *p*(WVDPM | WADPM) or not detecting a porpoise *p*(WVDPM | NOT WADPM).

Pearson's Chi-squared tests of goodness of fit were performed to test the significance of the mean values for these comparisons.

2.5.3 Calculating Click Difference of Arrival Times for Relative Depth Distribution

Synchronizing the hydrophones in a vertical array allowed for the calculation of the difference in arrival times (lag time) of a porpoise click detected by both receivers. Given the known distance between the two hydrophones (2.3m), depth of the midpoint of the array (~15m), and position of each hydrophone unit (upper or lower), the lag time in arrival was used as an assessment of porpoise depth distribution in the water column.

The analysis was completed using the MATLAB script, *classify_ici.m*. The dataset used for this analysis had no manually added detections (.trains) to ensure that all detections used had a strong signal strength. Only clicks that were recorded on both hydrophones could be used since the lag time was calculated by taking the difference in arrival times. Additionally, the minimum ICI considered was 0.01 seconds to ensure that detections across the hydrophones were of the same click.

The lag time equals the arrival time at the lower hydrophone minus the arrival time at the upper hydrophone. A negative lag time indicated a click being generated below the array midpoint (15 m) and a positive lag time indicated a click being generated from above the array midpoint. Appendix III models the error in meters associated with porpoise depth and range from the hydrophone array due to the error in the calculated lag times in click detection by both hydrophones.

Difference between the number of click pairs generated above and below the mid-point of the array was tested using a Chi-Square Test for Goodness of Fit. Difference in the mean sound levels (dB) detected above and below the hydrophone was tested using a Z-test.

2.5.4 Effect of Anthropogenic Noise

Short-duration anthropogenic noise in this study included three types; RHIB and speed boat, fishing vessels, and tidal turbine recovery operations. RHIB and speedboat included movements of small vessels, including the field vessel, that occurred during the sampling period. Fishing vessels included commercial fishing vessels observed during the sampling period. Tidal turbine recovery operations included all support vessels (mostly tug boats) and their movement during the removal of the Cape Sharp tidal turbine. Presence of anthropogenic noise in the data was

confirmed by manually cross checking the logbook observations of anthropogenic activities against spectrograms of acoustic recordings. The start and end times of an anthropogenic noise event was used to split the data into two groups (with and without activity).

2.5.5 Porpoise Detection Patterns (Time of Day / Location / Current Speed)

Comparisons of the porpoise detection patterns across time, space and current speed were carried out by sub setting the 1903 minutes of collected data into bins. DPM was the unit chosen for this analysis due to the high variability of inter-click intervals confounding the use of individual clicks as activity indicators. Data were binned by location (longitude), hour of the day (UTC), and signed current speed *s*

$$s = \text{sign}(u)\sqrt{u^2 + v^2} \qquad \text{(Eq. 1)}$$

Where u and v are easterly and northerly currents, respectively, in accordance with oceanographic convention.

Binning of hours was accomplished by taking the maximum and minimum time sampled (1500-2300 UTC) and dividing the hours into 4 bins of 2 hours each. Location bins were created by dividing the maximum and minimum longitude into three bins (Minas Channel, Minas Passage, and Minas Basin), taking into consideration bathymetry (Figure 5) and a power density model for the region (Karsten *et al.* 2008). The signed current speed (m/s) bins were -4.1 to -2.5, -2.5 to -1.0, -1.0 to 0.0, 0.0 to 1.0, 1.0 to 2.5, 2.5 to 4.6. A negative signed current speed with magnitude greater than 1 m/s meant the tide was in ebb phase. A signed current speed between -1.0 m/s and 1.0 m/s was defined as slack water. A signed current speed with a value greater than 1 m/s was considered flood phase.

Any minutes of recording that resided outside of the prescribed bins (I.e. small sample size < 100 minutes) were not included in the analysis.

The proportion *p* of DPM for each bin was determined by dividing the number of DPM in each cell by the number of total minutes in that cell:

$$p(DPM) = \frac{DPM}{N} \quad \text{(Eq. 2)}$$

Standard Error for categorical data was calculated for each *p*[DPM] using:

$$SEp(DPM) = \sqrt{\frac{p*(1-p)}{N}} \quad \text{(Eq. 3)}$$

A Pearson's Chi-squared test of goodness of fit was performed on each of the three factors to test if the observed distribution of DPM deviated significantly from the expected distribution of DPM. Where significance was shown, a post-hoc test (Pairwise Nominal Independence) was conducted.

It was observed that certain combinations of time of day, location and current speed were unequally sampled due to the design of our study. This lead to a directed analysis of current speed where average water column current speeds were investigated across location and time of day.

2.5.6 Calculating and Plotting Inter-Click Interval

The ICI characteristics were examined using the MATLAB program *classify_trains_by_ici.m* which recorded the temporal spacing of the clicks within a click train. Calculating the ICI values made use of all data containing manually added detections, as described in Section 2.4.

Additionally, given the large number of data points (14851 ICI values) and their wide range of values, a probability density function was used to plot all the ICI values

$$P_i = \frac{n_i}{N w_i} \quad \text{(Eq. 4)}$$

where n_i is the number of clicks within a bin, N is the total sample number, and w_i is the width of the bin.

Three modes were found in the initial ICI values (Figure 13). They were used to define ranges of ICI for three behaviors: navigation (> 10 ms), search (1 – 10 ms) and terminal/feeding buzz (< 1 ms). Once classed, individual trains were plotted to inspect fine detail in the porpoise click intervals.

3.0 RESULTS

All six drifter tracks converged when entering the narrow, fast moving water of Minas Passage and diverged when exiting the passage, either into Minas Channel or Minas Basin (Figure 5). The drifter was observed to largely follow the same track as the flotsam observed in Minas Passage.

Within the two-week field study period (12 – 27 June 2017), acoustic recordings were made during 1903 minutes over the course of 6 days. Of that active recording time no time was lost due to high flow noise. The Coda click detector identified 1269 minutes (67%) containing some evidence of porpoise echolocation clicks. After applying more stringent filters for signal to noise, click strength, and click train length, followed by a manual review process (Section 2.4), a total of 354 minutes (18.6%) contained strong evidence of the presence of harbour porpoise echolocation click trains. Within those minutes, 962 click trains were identified.

The opportunistic sampling of acoustic fish tags using the 69 kHz Vemco VR2W receivers resulted in no acoustic fish tag detections during the study period. Interestingly, the drifting icListenHF hydrophones detected a high resolution Vemco fish tag (180 kHz) over a 50-minute interval. The drifter mounted GoPro did not result in any footage of harbour porpoise, however, small unidentified fish were observed.

3.1 IcListenHF Hydrophone Performance

Synchronization of the two icListenHF hydrophones with respect to time allowed the porpoise detections from the two instruments to be compared. A total of 354 minutes (18.6%) of the total time sampled (1903 minutes) included click trains from at least one of the two hydrophone units.

First, we considered the question as to whether the upper icListenHF hydrophone (14 m) achieved greater or fewer detections than the lower instrument (16 m), regardless of unit number (1211 or 1239). Table 3 shows the mean number of clicks per minute (N = 354) detected by the upper and lower hydrophones and the results of the performed Z-test. The two hydrophones showed no significant difference in click detection rate with regard to vertical position on the drifter.

To test whether or not icListenHF 1211 performed differently from icListenHF 1239, average number of clicks per minute were compared, using data from: 1) each hydrophone regardless of vertical position, 2) times when icListenHF 1211 was in the upper position (N = 115 minutes, first two sampling days), and 3) times when icListenHF 1239 was in the upper position (N = 239 minutes, last four sampling days). Table 3 shows the average number of clicks detected per minute for each group compared and the results of the performed Z-tests. Although unit 1239 consistently showed higher mean click detection rates, the observed differences between units were not significant at $\alpha = 0.05$.

3.2 IcListenHF Hydrophone Detections vs Visual Observations

Visual observations of porpoises were made throughout the study area (Figure 8) and provided validation for the acoustic detection methods applied. While it is difficult to make comparisons between the visual sightings and acoustic detections of porpoises, acoustic detections are much more likely when there are visual detections than when there is no visual evidence of a porpoise. Similarly, visual sightings are much more likely when there are acoustic detections than when there is no acoustic evidence of porpoises. Table 4 shows clear statistical evidence that visual detections are more likely when there are acoustic detections and vice versa.

3.3 IcListenHF Hydrophones/Coda vs CPOD Detections

The icListenHF and Coda software detected approximately 16 times more DPMs than the CPODs (Table 5). Eleven DPMs were logged only by the CPOD. Upon further manual review of those eleven, three CPOD DPMs contained very weak porpoise clicks that were rejected by the Coda software. Of the other eight CPOD detections that were not also recorded by the icListenHF, none appeared to be porpoise clicks when closely examined; three contained broadband frequency spikes, two contained 69 kHz fish tag signals, one contained a 180 kHz echo sounder signal, and two contained no identifiable signals. Note that the 69kHz fish tags were used at test signals following drifter deployment. In contrast to CPODs, the icListenHF Coda does not mistake such signals for porpoise clicks.

Applying more stringent Coda filters and manually reviewing the icListenHF detections, to ensure accuracy in porpoise detections, had the effect of reducing the iclistenHF DPM detections from 1269 to 354 (Table 5). The comparison showed that the CPODs missed 85% of the stringently reviewed Coda DPM.

3.4 Patterns in Harbour Porpoise Detection

3.4.1 Porpoise Depth Distribution

Porpoise echolocation clicks were detected as being generated above or below the mid-point of the hydrophone array (15m) (Figure 9a). Of the paired detections, 14% more clicks were detected as being generated below 15 m than above (Table 6). Although the difference is statistically significant, one should not conclude much, if anything, from the statistical metric for at least three reasons:

1) The click detections above and below are similar enough that the observed difference may have little biological or physical relevance;

2) Measurements made at night may show a very different depth distribution; and

3) The depth of water column below 15 m varied during the drift surveys but always exceeded 15 m. Thus, any measurement error in time of arrival is more likely to bias results so that the number of clicks detected above 15 m is underestimated relative to the number below.

As expected, the mean sound levels (dB) for click pairs generated above and below the mid-point of the array were not significantly different (Table 7).

3.4.2 Detections in Relation to Anthropogenic Activity

Three types of short-term human activities (RHIB +speedboat, fishing vessels, and tidal turbine recovery operations) occurred during the study period. None had significant effects on the proportion of DPM detected during this study (Table 8). It is acknowledged, however, that the sample size (minutes) of observed anthropogenic activity was very low relative to "no activity" periods.

3.4.3 Detection Patterns (Time of Day/ Location/ Current Speed)

Proportions of DPM as a function of space (location), integrated across time and tidal phase, in Minas Channel and Minas Passage, were similar. Minas Basin had significantly lower proportions of DPM than Minas Passage and also the lowest average current speed (Figure 10; Table 9). The proportions of DPM as a function of time of day, integrated across space and tidal phase, demonstrated homogeneity across all the time bins except for the mid-day period (1500-1700 UTC) which had a significantly lower proportion of DPM and the lowest average current speed (Figure 11; Table 9**)**. The analysis on the current speed bins revealed significantly lower proportions of DPM during slack water periods (< 1 m/s) (Figure 12; Table 9). There was no significant difference in proportion of DPM among the faster current bins (> 1

m/s), regardless of tidal stage (ebb or flood). The highest mean proportion of DPM was in the > 2.5 m/s flood tide bin **(**Figure 12).

3.5 Inter-Click Interval

Probability density functions of the ICI revealed 3 distinct behavioral modes. Figure 13 highlights these modes by restricting the x and y axes. In this study, ICIs greater than 0.01 seconds are classified as navigation trains, ICIs between 0.01 and 0.001 seconds are classified as search trains and ICIs less than 0.001 second as a feeding buzz (Figure 13). Navigation behaviour was most commonly observed. Only 5 feeding buzzes were identified.

Closer examination of the ICIs within the search and feeding buzz modes showed a patterned structure with tightly spaced clusters of 2-4 clicks in 25% (4 of 16) of the search click trains and 4-5 clicks in most (4 of 5) of the feeding buzz click trains (Figure 14). No cluster patterns were observed in any of the navigation click trains examined.

4.0 DISCUSSION

4.1 Drifting Hydrophone Array Design

Hydrophones are effective tools for detecting harbour porpoise in high flow environments when flow noise is successfully mitigated. The custom design of the drifting hydrophone array in this study achieved this flow noise mitigation objective. Prior to this project, there have been only two reported studies on passive acoustic harbour porpoise monitoring using a drifting hydrophone in a high flow environment (Wilson *et al.* 2013; Benjamins *et al.* 2016). These studies used low cost porpoise echolocation loggers (CPODs) mounted to a Lagrangian drogue which could have resulted in acoustic contamination of CPOD datasets from surface waves. The present study showed CPODs to significantly underestimate porpoise activity (23%) when compared to the icListenHF hydrophone and Coda porpoise detection software.

This project took substantial steps to improve the drifter design and quality of acoustic measurements made using the drifting hydrophone array, including carefully isolating the hydrophones and using a specialized click detection system (newly developed Coda software). This was an improvement over a prior study in which stationary hydrophones were housed on a sensor platform in Minas Passage (Porskamp *et al.* 2015). That study experienced a 36% percent loss in CPOD recording time due to the CPOD memory buffer filling prematurely with flow noise; a co-deployed icListenHF was much less affected by high current speed (Porskamp *et al.* 2015). In contrast, our drifting array of icListenHF hydrophones and CPODs experienced no flow noise effects and no lost CPOD recording time.

In prior CPOD studies in Minas Passage, spatial and temporal variation in porpoise activity was detected by deploying CPODs within tethered SUBs at multiple

sites in and near the FORCE crown lease area (Tollit *et al.* 2011, Wood *et al.* 2013). This process was labour intensive, required a vessel capable of deploying many moorings, and also assumed that all click detectors (CPODs) would be operational throughout the study period and with the same performance level. Unfortunately, the CPODs frequently malfunctioned for unknown reasons. The design used in the present study included a single drifting platform that sampled as it moved in and out of Minas Passage. This allowed comparison of porpoise activity as the drifter moved within tidal waters across three areas: Minas Channel, Minas Passage, and Minas Basin. Presently, we have no way to remotely monitor the drifter, so its application requires considerable personnel time, but it does offer opportunities for acoustic detection validation via concurrent visual observations.

The collection of high resolution GPS drifter tracks provided key data for the present study and can be used to inform future studies on surface flow dynamics in the area. Additionally, the drifter tracks confirm the location of debris fields within Minas Passage and may be useful for diagnosing the mechanics of this surface convergence.

4.2 Click Detections, Visual Observations, and Anthropogenic Activity

The accuracy of marine mammal detections using passive acoustic monitoring technology is often questioned when there are no visual sightings to confirm the presence of a vocalizing marine mammal. Visual sightings of harbour porpoise were common during the study period, and the probability of acoustically detecting porpoises (WADPM) was positively related to the probability of visually observing porpoises (WVDPM). This is consistent with the findings of a drifter survey completed by Wilson *et al.* (2013) on the west coast of Scotland, where CPOD detections of porpoise click trains were supported by visual surveys.

A drawback with visual observation methods is that it requires observers to be vigilant for extended periods of time. Deteriorating weather conditions and observer fatigue can make continuous visual observations difficult. However, the indisputable benefit of visual surveys is the identification of the species and counts of individuals, which is not possible with the acoustic methods employed in Minas Passage but would be possible with an array of at least four hydrophones.

The finding that short duration anthropogenic noise had no observable effect on harbour porpoise echolocation activity is contrary to observations by Koschinski *et al.* (2003), who observed increases in harbour porpoise echolocation activity when porpoises were exposed to simulated anthropogenic noise, in that case a 2 MW wind power generator. An explanation for our observation of no effects could be that harbour porpoises in Minas Passage were only briefly exposed to the noise of watercraft. Additionally, the small sample size (minutes) during which there was anthropogenic noise within our study did not provide enough data to reach a definitive conclusion.

4.3 DPM Patterns with Location, Time of Day, and Current Speed

The drifting array inextricably linked location, time of day and current speed. Due to weather, tide and daylight constraints, and the nature of a drifting array, certain combinations of time, location, and current speed were sampled unequally, while some were not sampled at all (Appendix II). As these constraints caused aliasing across the results, the effects of each factor were considered independently.

The analysis of activity across time of the day (2-hour bins) showed higher detections in the afternoon to evening hours (1700-2300 UTC). A prior series of baseline passive acoustic studies in Minas Passage (Tollit *et al.* 2011, Wood *et al.*

2013), that were subsequently modelled (GAM/GEE) by Porskamp (2015) indicated a similarly depressed level of echolocation activity at mid-day, with increased activity toward dusk.

Surprisingly, our study indicated low porpoise activity at low current speeds (< 1 m/s). This result is in sharp contrast to multi-year CPOD field data and GAM/GEE model results (Porskamp *et al.* 2015), which indicated elevated porpoise echolocation activity at low current speeds (at and near slack water). An explanation for this incongruence is that the tethered SUB buoys that are used to moor CPODs at / near FORCE contributed to elevated noise levels during flood and ebb tides, and consequently reduced CPOD efficiency and performance during high flow periods. Additionally, tidal stage trends in porpoise activity, shown by Porskamp *et al.* (2015), indicate a west-east gradient, with porpoises moving into Minas Passage from Minas Channel on the flood tide, thus elevating the likelihood of CPODs detecting porpoise clicks in Minas Passage during high tide slack water periods.

4.4 Porpoise Depth Distribution

Porpoise depth distribution has implications for tidal energy development in Minas Passage and potential turbine-porpoise interactions. The observed click detections both above and below 15 m suggests that porpoises will spatially overlap with a wide range of tidal energy turbine designs proposed for installation in Minas Passage. Such interactions could be physical (e.g. collision) or behavioral (e.g. avoidance), and these could result in changes in porpoise use of the area. Due to the limitations of the two-hydrophone array, only a rough approximation of porpoise depth distribution could be calculated (above or below 15 m). Additional work is planned to expand the hydrophone array to study in detail porpoise depth distribution in Minas Passage and associated risks from turbine installations.

4.5 Harbour Porpoise Behaviour Indicators

Examination of porpoise inter-click intervals (ICI) offered insight into porpoise behaviour during the study period. The observed modes of ICI suggest that porpoises were engaged in three main behaviours which were classified as navigation (ICI > 10 ms), search (ICI ~ 1 – 10 ms) and feeding buzz (ICI < 1 ms) (Figure 13). The ICI ranges and behavioural classifications differ from those of Verfuß *et al.* (2009) where the echolocation trains of two trained porpoises in a 36 m×15 m semi-natural outdoor enclosure in Denmark were recorded and analyzed. Verfuß *et al.* (2009) delineated observed ICIs into search phase (ICI > 50 ms), approach phase (ICI <50 ms), and feeding buzz (~1.5 ms). The effects of confining porpoises to an enclosure on behaviour and associated ICIs is unknown. It is also possible that ICI varies among different porpoise populations.

A unique finding of this study was the observation of patterned structure in click sequences, with tightly spaced clusters of 2-5 clicks within the majority of click trains that were classed as feeding buzzes (Figure 14). Clustered clicks were only sometimes (25%) observed in search trains (Figure 14) and were never observed in navigation trains. A possible explanation is that the closely grouped clicks are a result of the air bouncing between the air sacs within the acoustic production center of the nasal complex. As the ICI decreases, the muscles may have less time to relax resulting in the incidence of travelling air on a membrane under tension, thus being directed back through the phonic lips using elastic energy. Whether these secondary clicks are functionally used by the porpoise to increase the resolution of its acoustic image is unknown.

5.0 CONCLUSIONS

The design of the drifting hydrophone array used in Minas Passage served to mitigate the effects of flow noise and surface waves. High quality acoustic data (1903 minutes over six days) was successfully analyzed using the newly developed Coda click detector and associated filters. The porpoise detection results from the drifting array of hydrophones were supported by contemporaneous visual observations of harbour porpoise during the drift surveys. The effects of short-duration anthropogenic noise from fishing vessels and other boat traffic were found to have no observable effect on porpoise activity. The Coda detector was effective in investigating novel patterns in the inter-click interval of porpoise echolocation clicks. Various behaviours, including feeding, searching and navigation, were identified. Additionally, the detection positive minutes show patterns in porpoise activity in relation to time of day, location and current speed. Porpoise activity was relatively low in Minas Basin, during early afternoon (1500-1700 UTC) and when current speed was slow (<1 m/s). Lastly, the multi-hydrophone array confirmed porpoise use of the water column both above and below 15 m. A larger hydrophone array will be necessary to acquire precise depth distribution and range, and also estimates of porpoise density.

6.0 RECOMMENDATIONS FOR FUTURE STUDY

The work completed in this project will be used to inform future work on harbour porpoise behavior and interactions with tidal energy developments in Minas Passage. Continued use of drifters should incorporate a greater number of synced hydrophones in the array (up to six units), thus allowing for localization of porpoises in 3D space (precise depth and range). The hydrophones should be drifted both through and near the FORCE test site, before and after the next deployment of a tidal turbine. Before and after trends in porpoise detection and depth distribution can then be used to assess the effect of an operational turbine on porpoise behavior (e.g. avoidance or attraction). Moreover, it may be possible to attribute echolocation clicks to an individual porpoise, which would then allow determination of the density of porpoises close to and away from the turbine. Such results are recommended for estimating porpoise-turbine encounter rate.

To extend the usefulness of this project, future drifter-based projects in high flow environments should ensure that the study is carefully designed to equally and amply distribute sampling effort to fully explore how click detections are related to time, location and current speed. Ideally, the drifter would be deployed for 24-hour periods, which may be possible due to the tidal dynamics of Minas Passage and adjacent areas, where drifters are known to remain within the inner Bay of Fundy for multiple weeks (NOAA 2017).

REFERENCES

Ainslie M. A. & McColm J. G. 1998. A simplified formula for viscous and chemical absorption in sea water. Journal of the Acoustical Society of America **103**(3): 671-1672.

Au, W. L. 1999. Transmission beam pattern and echolocation signals of a harbour porpoise (*Phocoena phocoena)*. The Journal of the Acoustical Society of America **106**: 3699.

Audacity. 2017. Version 2.1.2. User Manual.

Bannister, J. L. 2009. Baleen Whales (Mysticetes). Encyclopedia of Marine Mammals **2**: 82-88.

Benjamins, S., Dale, A., van Geel, N., and Wilson, B. 2016. Riding the tide: use of a moving tidal-stream habitat by harbour porpoises. Marine Ecology Progress Series **549**: 275-288.

Bjørge, A. and Tolley, K. A., 2009. Harbor Porpoise (*Phocoena phocoena*). Encyclopedia of Marine Mammals **2**: 530-532.

Brandt M. J., Diederichs A., Betke K., Nehls G. 2011. Responses of harbour porpoises to pile driving at the Horns Rev II offshore wind farm in the Danish North Sea. Marine Ecology Progress Series **421**: 205-216.

Buckstaff, K. C. 2004. Effects of watercraft noise on the acoustic behavior of bottlenose dolphins, *Tursiops truncatus*, in Sarasota Bay, Florida. Marine Mammal Science, **20**(4): 709-725.

Codarin, A., Wysocki, L. E., Ladich, F., and Picciulin, M. 2009. Effects of ambient and boat noise on hearing and communication in three fish species living in a marine protected area (Miramare, Italy). Marine Pollution Bulletin **58**(12): 1880-1887.

COSEWIC. 2006. COSEWIC assessment and update status report on the harbour porpoise *Phocoena phocoena* (Northwest Atlantic population) in Canada. Committee on the Status of Endangered Wildlife in Canada. Ottawa. vii [www.sararegistry.gc.ca/status/status_e.cfm]

COSEWIC. 2008. COSEWIC assessment and update status report on the killer whale *Orcinus Orca*, Southern Resident Population, Northern Resident Population, West Coast Transient Population, Offshore Population and Northwest Atlantic / Eastern Arctic Population, in Canada. Committee on the Status of Endangered Wildlife in Canada. Ottawa.

Evans D. L., England G. R., Lautenbacher, C. C., Hogarth, W. T., Livingstone, S. M., and Johnson, H. T. 2001. Bahamas marine mammal stranding event of 15-16 March 2000. Joint Interim Report (National Oceanic and Atmospheric Administration and Department of the Navy).

Fader, G. 2009. Geological report for the proposed in stream tidal power demonstration project in Minas Passage, Bay of Fundy, Nova Scotia. Atlantic Marine Geological Consulting Ltd, Halifax, NS.

Filezilla. 2018. Version 3.30.0

Fisher F. H. & Simmons V. P. 1977. Sound absorption in seawater. Journal of the Acoustical Society of America **62**: 558-564.

Fogarty, L. C. 2012. Listening in the fast lane: detecting Harbour Porpoise activity in the Minas Passage. Honours thesis, Acadia University, Wolfville, NS.

Foote, A.D., Osborne, R.W., & Rus Hoelzel, A. 2004. Whale-call response to masking boat noise. Nature (London) **428**: 910.

Francois R. E. & Garrison G. R. 1982a. Sound absorption based on ocean measurements: Part I: Pure water and magnesium sulfate contributions. Journal of the Acoustical Society of America **72**(3): 896-907.

Francois R. E. & Garrison G. R. 1982b. Sound absorption based on ocean measurements: Part II: Boric acid contribution and equation for total absorption. Journal of the Acoustical Society of America 72(6): 1879-1890.

Garmin Ltd. 2016. Garmin Basecamp Software. Version 4.6.2.

Garmin Ltd. 2011. GPSMAP 62 series Owner's Manual. Garmin.

Gaskin, D.E. 1984. The harbour porpoise *Phocoena phocoena* (L.): regional populations, status, and information on direct and indirect catches. Reports of the International Whaling Commission **34**: 569-586.

Gaskin, D.E. 1992. Status of the harbour porpoise, *Phocoena phocoena*, in Canada. Canadian Field-Naturalist 196: 36-54.

Goodson, A.D., and Sturtivant, C.R. 1996. Sonar Characteristics of the Harbour Porpoise (*Phocoena Phocoena*): Source Levels and Spectrum. ICES Journal of Marine Science **53**: 465-472.

Griffin, D. R., Webster, F. A., and Michael, C. R. 1960. The echolocation of flying insects by bats. Animal Behaviour 8: 141-154.

Hildebrand, J. A. 2009. Anthropogenic and natural sources of ambient noise in the ocean. Marine Ecology Progress Series **395**: 5-20.

Jones, M. L., Swartz, S. L., & Dahlheim, M. E. 1994. Census of gray whale abundance in San Ignacio Lagoon: a follow-up study in response to low whale counts recorded during an acoustic playback study of noise effects on gray whales. Report to the U.S. Marine Mammal Commission, Washington, DC. NTIS PB94195062.

Karsten, R., McMillan, J., Lickley, M., and Haynes, R. 2008. Assessment of tidal current energy in the Minas Passage, Bay of Fundy. Journal of Power and Energy **222**: 493-507

Kastelein, R.A., Bunskoek, P., Hagedoorn, M., Au, W.L.W. & de Haan, D. 2002. Audiogram of a harbor porpoise (*Phocoena phocoena*) measured with narrow-band frequency-modulated signals. Journal of the Acoustical Society of America **112**(1): 334-344.

Koschinski, S., Culik, B. M., Henriksen, O. D., Tregenza, N., Ellis, G., Jansen, C., Kathe, G. 2003. Behavioural reactions of free-ranging porpoises and seals to the noise of a simulated 2 MW windpower generator. Marine Ecology Progress Series **263**: 263-273.

Koschinski, S., Diederichs, A., Amundin, M., 2008. Click train patterns of free-ranging Harbour Porpoises acquired using T-PODs may be useful indicators of behaviour. Journal of Cetacean Research and Management, **10**(2): 147-155.

Lesage, V., Barrette, C., Kingsley, M. C. S., & Sjare, B. 1999. The effect of vessel noise on the vocal behavior of belugas in the St. Lawrence River Estuary, Canada. Marine Mammal Science **15**(1): 65-84.

Li, H., Deng, Z. D., Carlson, T. J. 2002. Piezoelectric materials used in underwater transducers. Sensor Letters. Energy and Environment Directorate, Pacific Northwest National Laboratory, P.O. Box 999, Richland, Washington 99352, USA.

Mann, D.A., Z. Lu, and A.N. Popper. 1997. A clupeid fish can detect ultrasound. Nature 389-341.

Martin, B. and L. Horwich. 2017. Acoustic Data Analysis of the OpenHydro Open Center Turbine at FORCE – Phase 1 Report. Document 01516, Version 1.1 DRAFT. Technical report by JASCO Applied Sciences for Cape Sharp Tidal.

MATLAB and Statistics Toolbox Release 2016a. 2016. The MathWorks, Inc., Natick, Massachusetts, United States.

Medwin, H. 1975. Speed of sound in water: a simple equation for realistic parameters. Journal of the Acoustical Society of America **58**: 1318-1319.

Melcón, M. L., Denzinger, A., and Schnitzler, H.-U. 2007. Aerial hawking and landing: approach behaviour in Natterer's bats, *Myotis nattereri* (Kuhl 1818). Journal of Experimental Biology **210**: 4457-4464.

Nedwell, J. R., Edwards, B., Turnpenny, A.W. H., and Gordon, J. 2004. Fish and marine mammal audiograms: A summary of available information. Prepared by Subacoustech Ltd., Hamphire,UK. Report 534 R 0214.

Nowacek, D. P., Thorne, L. H., Johnston, D. W., and Tyack, P. L. 2007. Responses of Cetaceans to Anthropogenic Noise. Mammal Review **37**: 81–115. doi:10.1111/J.1365-2907.2007.00104.X

NOAA. 2017. GOMI surface drifter tracks in Bay of Fundy. Northeast Fisheries Science Centre. https://www.nefsc.noaa.gov/drifter/drift_gomi_2017_2.html [accessed 13 March 2018].

OceanSonics. 2017a. Choosing Best Sample Rate [online]. Available from http://oceansonics.com/wp-content/uploads/Choosing-the-Best-Hydrophone-Sample-Rate1.pdf [accessed 14 April 2017].

OceanSonics. 2017b. What is a Smart Hydrophone? [online]. Available from http://oceansonics.com/what-is-a-smart-hydrophone/ [accessed 14 April 2017].

OceanSonics. 2017c. Arrays. [online] Available from http://oceansonics.com/arrays/ [accessed 22 April 2017].

OEER Association. 2008. Fundy Tidal Energy Strategic Environmental Assessment. Nova Scotia Department of Energy.

Palka, D. 1996. Effects of Beaufort sea state on the sightability of harbor porpoises in the Gulf of Maine. Report of the International Whaling Commission **46**: 575–582.

Porskamp, P. H. J. 2015. Detecting and assessing trends in harbour porpoise (*Phocoena phocoena)* presence in and around the FORCE test site. Acadia University, Wolfville, NS.

Porskamp, P. H. J., Redden, A.M., Broome. J., Sanderson, B., and Wood, J. 2015. Assessing marine mammal presence in and near the FORCE Lease Area during winter and early spring – addressing baseline data gaps and sensor performance. Report to the Offshore Energy Research Association and FORCE. ACER Technical Report No 121, 35 pp. Acadia University, Wolfville, NS, Canada.

R Core Team. 2016. R: A language and environment for statistical computing. R Foundation for Statistical Computing, Vienna, Austria. URL https://www.R-project.org/.

Recchia, C.A., and Read, A.J. 1989. Stomach contents of harbour porpoises, *Phocoena phocoena* (L.), from the Bay of Fundy. Canadian Journal of Zoology **67**: 2140-2146.

Richardson, W. J., Greene Jr, C. R., Malme, C. I., Thomson, D, H. 1995. Marine mammals and noise. Academic Press.

Romano, T. A., Keogh, M. J., Kelly, C., Feng, P., Berk, L., Schlundt, C. E., Carder, D. A., & Finneran, J. J. 2004. Anthropogenic sound and marine mammal health: measures of the nervous and immune systems before and after intense sound exposure. Canadian Journal of Fisheries and Aquatic Sciences 61: 1124-1134.

Sanderson, B., Buhariwalla, C., Adams, M., Broome, J., Stokesbury, M., and Redden, A. 2017. Quantifying detection range of acoustic tags for probability of fish

encountering MHK devices. European Wave and Tidal Energy (EWTEC) 2017 Conference. Cork, Ireland. 10 pp.

Scheifele, P. M., Andrew, S., Cooper, R. A., Darre, M., Musiek, F. E., & Max, L. 2005. Indication of a Lombard vocal response in the St. Lawrence River beluga. Journal of the Acoustical Society of America 117(3): 1486-1492.

Smith, R. J. and Read A. J. 1992. Consumption of euphausiids by harbour porpoise (*Phocoena phocoena*) calves in the Bay of Fundy. Canadian Journal of Zoology **70**: 1629-1632.

Strasberg, M. 1985. Hydrodynamic flow noise in hydrophones. H.G. Urban (ed.) Adaptive Methods in Underwater Acoustics 125-143.

Stewart, P., Lavender, F., and Maclean, M. 2013. Observations of harbour porpoise (*Phocoena phocoena*) at the Fundy tidal energy demonstration site Minas Passage, Nova Scotia – 2009-2012. Poster presented at the 2013 Nova Scotia Tidal Energy Research Symposium and Forum, May 14-15, 2013, Wolfville, Nova Scotia.

Thompson, P. M., Brookes, K. L., Graham, I. L., Barton, T. R., Needham, K., Bradbury, G., and Merchant, N.D. 2013. Short-term disturbance by a commercial two-dimensional seismic survey does not lead to long-term displacement of harbour porpoises. Proceedings of the Royal Society. **280**: 20132001. http://dx.doi.org/10.1098/rspb.2013.2001.

Thorne, P. 1987. Laboratory and marine measurements on the acoustic detection of sediment transport. Journal of the Acoustical Society of America 80: 899-910.

Tollit, D., Wood, J., Broome, J., and Redden, A. 2011. Detection of marine mammals and effects monitoring at the NSPI (OpenHydro) turbine site in the Minas Passage during 2010. Prepared for Fundy Ocean Research Centre for Energy.

Tyack, P.L. 2008. Implications for marine mammals of large-scale changes in the marine acoustic environment. Journal of Mammalogy **89**(3): 549-558.

Varshney, L. R., and Sun, J. Z. 2013. Why do we perceive logarithmically? Significance **10**(1): 28-31.

Verfuß, U., Miller, L., Pilz, P., and Schnitzler, H. 2009. Echolocation by two foraging harbour porpoises (*Phocoena phocoena*). Journal of Experimental Biology **212**: 823-834.

Villadsgaard, A., Wahlberg, M., and Tougaard, J. 2007. Echolocation signals of wild harbour porpoises, *Phocoena phocoena*. Journal of Experimental Biology **210**: 56-64.

Wahlberg, M., Linnenschmidt, M., Madsen, P., Wisniewska, D., Miller, L. 2015. The acoustic world of the harbor porpoise. American Scientist **103**(1): 46.

Weilgart, L. S. 2007. The impacts of anthropogenic ocean noise on cetaceans and implications for management. Canadian Journal of Zoology **85**: 1091-1116.

Wilson, B., Benjamins, S., and Elliot, J. 2013. Using drifting passive echolocation loggers to study harbour porpoises in tidal-stream habitats. Endangered Species Research **22**: 125-143.

Wood, J., Tollit, D., Redden, A. Porskamp, P., Broome, J., Fogarty, L., Booth, C., and Karsten, R. 2013. Passive acoustic monitoring of cetacean activity patterns and movements in Minas Passage: Pre-turbine baseline conditions (2011-2012). Final Report for Fundy Ocean Research Centre for Energy (FORCE) and Offshore Energy Research Association (OERA), Halifax, NS.

Zimmer, W. M. X. 2011. Passive acoustics monitoring of cetaceans. University Printing House, Cambridge, United Kingdom.

TABLES

Table 1. Examples of common anthropogenic noise contributors and their characteristics. V = vertical, H = horizontal, CW = constant wave (Codarin *et* al 2009; Hildebrand 2009).

Sound source	Source (dB re 1 µPa @ 1 m)	Bandwidth Δ = 10 dB (Hz)	Source direction	Pulse duration (s)
Torpedo MK-46 (98 lb explosive)	289	10–200	Omni	0.1
Air-gun array	260	5–300	60 × 180° V	0.03
US Navy 53C ASW sonar	235	2k–8k	40 × 360° H	2
Pile-driving 1000 kJ hammer	237	100–1k	15 × 360° H	0.05
Multibeam sonar shallow EM 710	232	70k–100k	0.5 × 140° V	0.002
Cargo vessel (173 m length, 16 knots)	192	40–100	80 × 180°	CW
Small boat (outboard engine, 20 knots)	160	1k–5k	80 × 180°	CW
Fishing vessel (163 HP diesel engine, 6 knots)	138	0.3k-10k	80 x180°	CW

Table 2. Advantages and disadvantages of various hydrophone deployment methods.

Deployment Methods	Advantages	Disadvantages
Instrument platforms (Cabled or Autonomous)	• Long temporal coverage (requires power) • Fixed position and tilt • Real-time data if cabled • Cabled option eliminates battery power and data storage constraints	• Small spatial coverage • Flow noise may be an issue at high current speeds • Deployment and retrieval is labor intensive
Tethered using SUBS mooring (near bottom floats)	• Equipment position remains somewhat stationary • Long temporal coverage	• Small spatial coverage • Flow noise is an issue at high current speeds • Instrument tilt varies • Deployment and retrieval is labor intensive
Stationary array on turbine infrastructure	• Eliminates power and data storage constraints • Long temporal coverage	• Noise from infrastructure may contaminate acoustic data • Limited opportunity for instrument maintenance • Flow noise becomes an issue at high current speeds • Small spatial coverage
Towed array	• Realtime data • Multiple hydrophones allow for detection localization • Directed spatial coverage (e.g. transects)	• Vessel / personnel required for tows • Vessel noise • Flow noise • Short temporal coverage
Drifting array	• Relatively low cost • Large spatial coverage • Instrument moving with current mitigates flow noise	• Short temporal coverage • Requires attendant boat/personnel • Pressure fluctuations due to wave action may become an issue (but can be mitigated)

Table 3. Hydrophone unit and vertical position comparisons. For each instrument the number of detections was calculated during each of the 1903 minutes sampled over six days. Of these, 354 minutes were selected as containing high-quality harbour porpoise clicks detected by at least one of the two hydrophones. Comparisons of detection performance (mean number of detections per minute ± SE) were performed using Z-tests. Upper position = 14m depth and lower = 16m depth. Note: Unit 1211 was positioned at the upper position for the first two deployment days while unit 1239 was positioned at the upper position for the last four deployment days.

Comparison	Specification	Mean (Standard Error)		Z-score	P-value $\alpha = 0.05$
		Upper	Lower		
Position (upper vs lower)	Regardless of unit	17.05 (1.74)	15.95 (1.61)	0.46	0.65
		#1211	#1239		
Hydrophone Unit (1211 vs 1239)	Regardless of position	15.13 (1.14)	17.87 (1.23)	-1.15	0.25
	1211 at upper position	13.30 (1.71)	15.83 (1.72)	-0.74	0.46
	1239 at upper position	16.02 (2.12)	18.85 (1.89)	-1.00	0.32

Table 4. Comparison of proportions of click train detections in windowed acoustic detection positive minutes (WADPM) in relation to windowed acoustic visual detection positive minutes (WVDPM). SE is the standard error. The p-values are the results of a Post-Hoc (Pairwise Nominal Independence) tests on Chi-Square tests performed on the correlation between acoustic and visual detections.

Variable	Proportion Mean (SE)	N (min)	P-value $\alpha = 0.05$
WADPM | WVDPM	0.32 (0.02)	375	< 0.001
WADPM | not WVDPM	0.15 (0.009)	1528	
WVDPM | WADPM	0.29 (0.01)	1010	< 0.001
WVDPM | not WADPM	0.09 (0.01)	893	

Table 5. Harbour porpoise DPM for CPODs and icListenHF hydrophones, with and without stringent Coda filters. The stringent Coda filters included signal to noise, click strength, and click train length filters, followed by a manual review process (see Section 2.4).

Detector	# of DPM (of 1903 min of acoustic data) without Coda filters	# of DPM with stringent Coda filters
icListenHF all detections	1269	354
icListenHF (no CPOD DPM)	1199	301
CPOD all detections	81	81
CPOD (with icListenHF DPM)	70	53
CPOD (no icListenHF DPM)	11	28

Table 6. Comparison of paired harbour porpoise clicks detected by both icListenHF hydrophones as being generated above or below the mid-point of the drifting hydrophone array (15 m) using a Chi-square Test for Goodness of Fit.

Paired Click Origin	N (Paired Detections)	Chi Square value	P-value $\alpha = 0.05$
Above mid-point of array	969	9.05	0.003
Below mid-point of array	1106		

Table 7. Comparison of mean sound levels (dB) of paired porpoise clicks detected by both icListenHF hydrophones as being generated above or below the midpoint of the array (15 m) using a Z-test. N = number of clicks.

Paired Click Origin	Mean dB (Standard Error)	N	Z-value	P-value $\alpha = 0.05$
Above mid-point of array	125.33 (0.31)	969	0.84	0.40
Below mid-point of array	124.98 (0.27)	1106		

Table 8. Comparison of icListenHF detection positive minutes (DPM) with and without anthropogenic activities. RHIB denotes the rigid hull inflatable boat used as the field vessel. N is the number of minutes sampled. SE is the standard error. The p-values are the result of Post-Hoc (Pairwise Nominal Independence) tests on the Chi-Square test performed on the three analyzed factors of anthropogenic activity.

Anthropogenic Activity	DPM with activity Proportion (SE) N	DPM with no activity Proportion (SE) N	P-value $\alpha = 0.05$
RHIB + speedboat	0.15 (0.03) 137	0.19 (0.03) 1766	0.364
Fishing Vessels	0.19 (0.05) 57	0.19 (0.01) 1866	1.00
Tidal Turbine Retrieval	0.29 (0.07) 41	0.18 (0.01) 1862	0.116

Table 9. Post-Hoc (Pairwise Nominal Independence) tests on the Chi-Square tests performed on the three analyzed factors (time, location, and current speed) which compared the proportions of DPMs within the minutes sampled for the bin. N is the number of minutes sampled.

Factor	Comparison	N	P-value $\alpha = 0.05$
Location	Minas Basin vs. Minas Channel	299 vs. 963	0.075
	Minas Basin vs. Minas Passage	299 vs. 641	0.016
	Minas Channel vs. Minas Passage	963 vs. 628	0.158
Time	1500 – 1700 vs. 1700 – 1900	360 vs. 492	< 0.001
	1500 – 1700 vs. 1900 – 2100	360 vs. 657	0.009
	1500 – 1700 vs. 2100 – 2300	360 vs. 309	0.036
	1700 – 1900 vs. 1900 – 2100	492 vs. 657	0.455
	1700 – 1900 vs. 2100 – 2300	492 vs. 309	0.455
	1900 – 2100 vs. 2100 – 2300	657 vs. 309	0.833
Current Speed	< -2.5 vs. > 2.5	255 vs. 230	0.230
	< -2.5 vs. 0.0 to 1.0	255 vs. 428	0.006
	< -2.5 vs. 1.0 to 2.5	255 vs. 564	0.977
	< -2.5 vs. -1.0 to 0.0	255 vs. 132	0.237
	< -2.5 vs. -2.5 to -1.0	255 vs. 294	0.977
	> 2.5 vs. 0.0 to 1.0	230 vs. 428	< 0.001
	> 2.5 vs. 1.0 to 2.5	230 vs. 564	0.229
	> 2.5 vs. -1.0 to 0.0	230 vs. 132	0.025
	> 2.5 vs. -2.5 to -1.0	230 vs. 294	0.248
	0.0 to 1.0 vs. 1.0 to 2.5	428 vs. 564	0.004
	0.0 to 1.0 vs. -1.0 to 0.0	428 vs. 132	0.622
	0.0 to 1.0 vs. -2.5 to -1.0	428 vs. 294	0.002
	1.0 to 2.5 vs. -1.0 to 0.0	564 vs. 132	0.206
	1.0 to 2.5 vs. -2.5 to -1.0	564 vs. 294	1.00
	-1.0 to 0.0 vs. -2.5 to -1.0	132 vs. 294	0.229

FIGURES

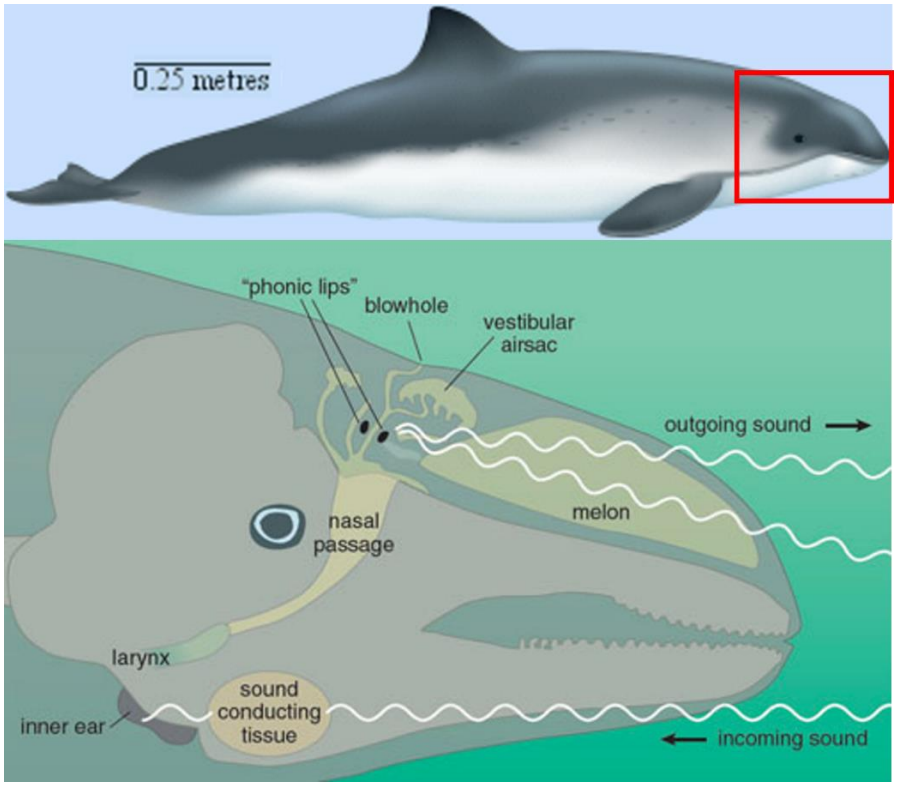

Figure 1. Top: Atlantic harbour porpoise, *Phocoena phocoena*, sideview. Bottom: Vocalization structures of a harbour porpoise (Wahlberg et al 2015).

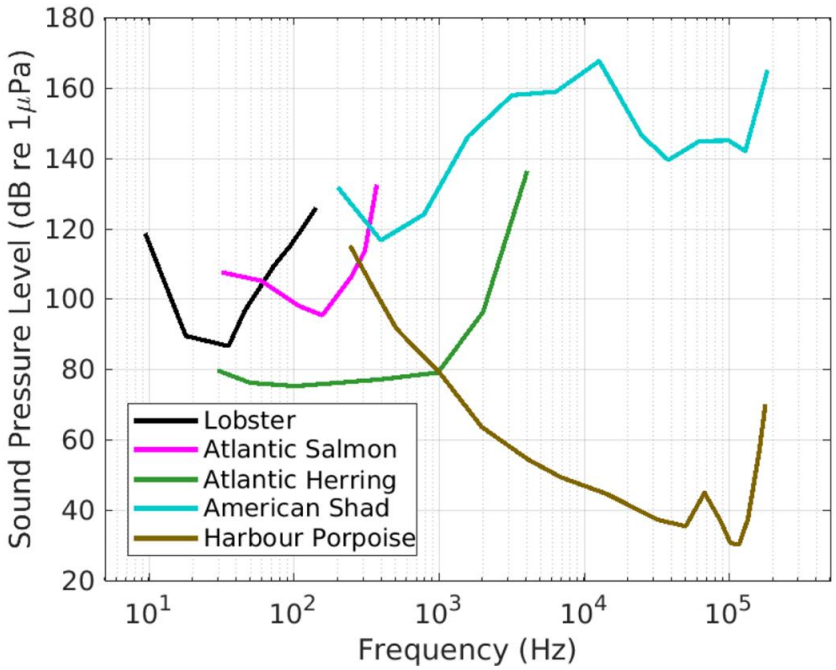

Figure 2. Audiograms generated for five species common to the Minas Passage and surrounding waters. Note log scale on x-axis. See review in Nedwell *et al.* 2004.

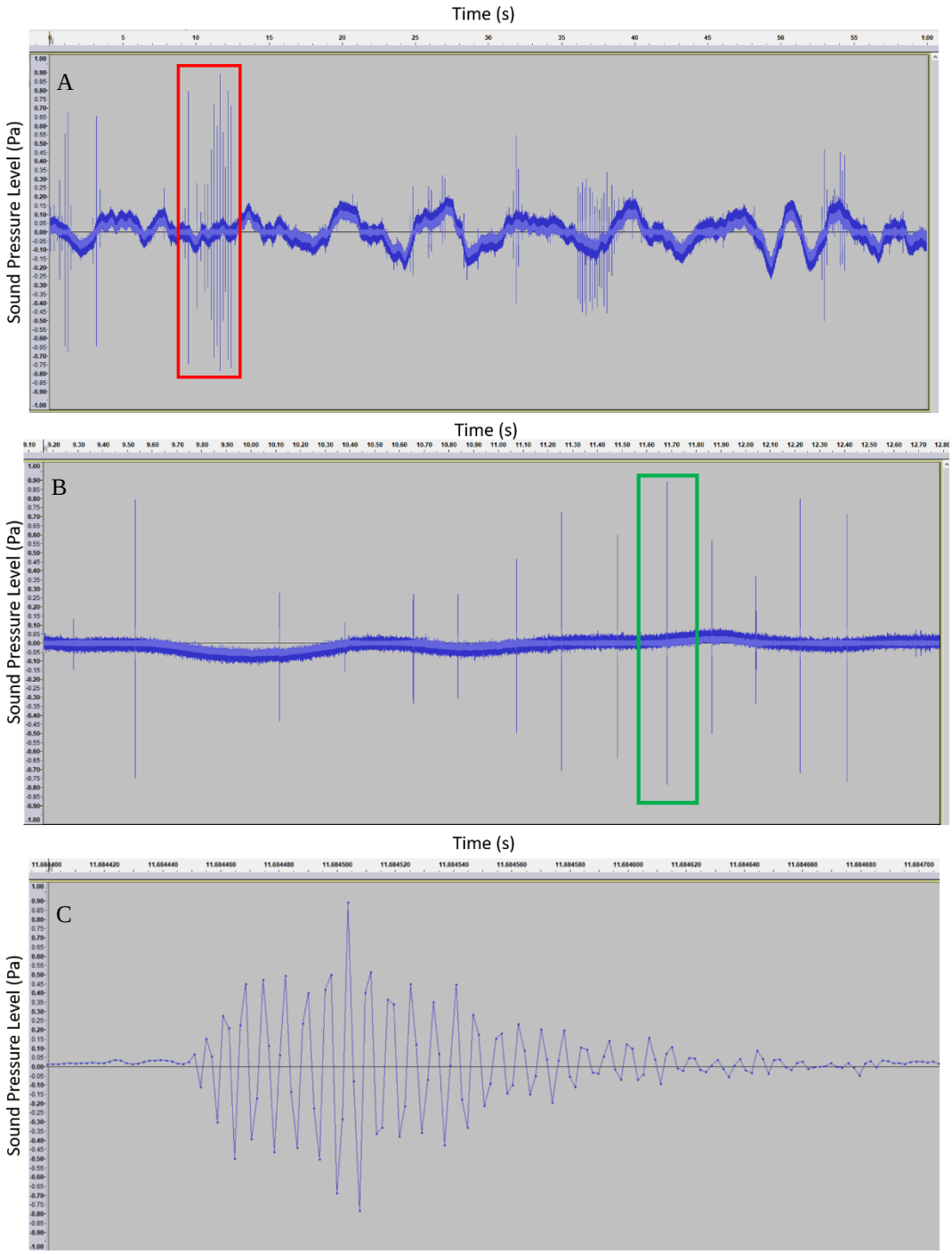

Figure 3. Example screenshots. Plot A is a one-minute time-series/waveform generated using Audacity (2017) from data collected using an IcListenHF hydrophone mounted on a drifter in Minas Passage, at 1300h on October 7th, 2016. The top x-axis denotes time (s), the y-axis denotes pressure level (Pa) normalized to 1.00. The red box indicates a harbour porpoise click train which is highlighted in plot B. The green box indicates the single harbour porpoise click which is highlighted in plot C.

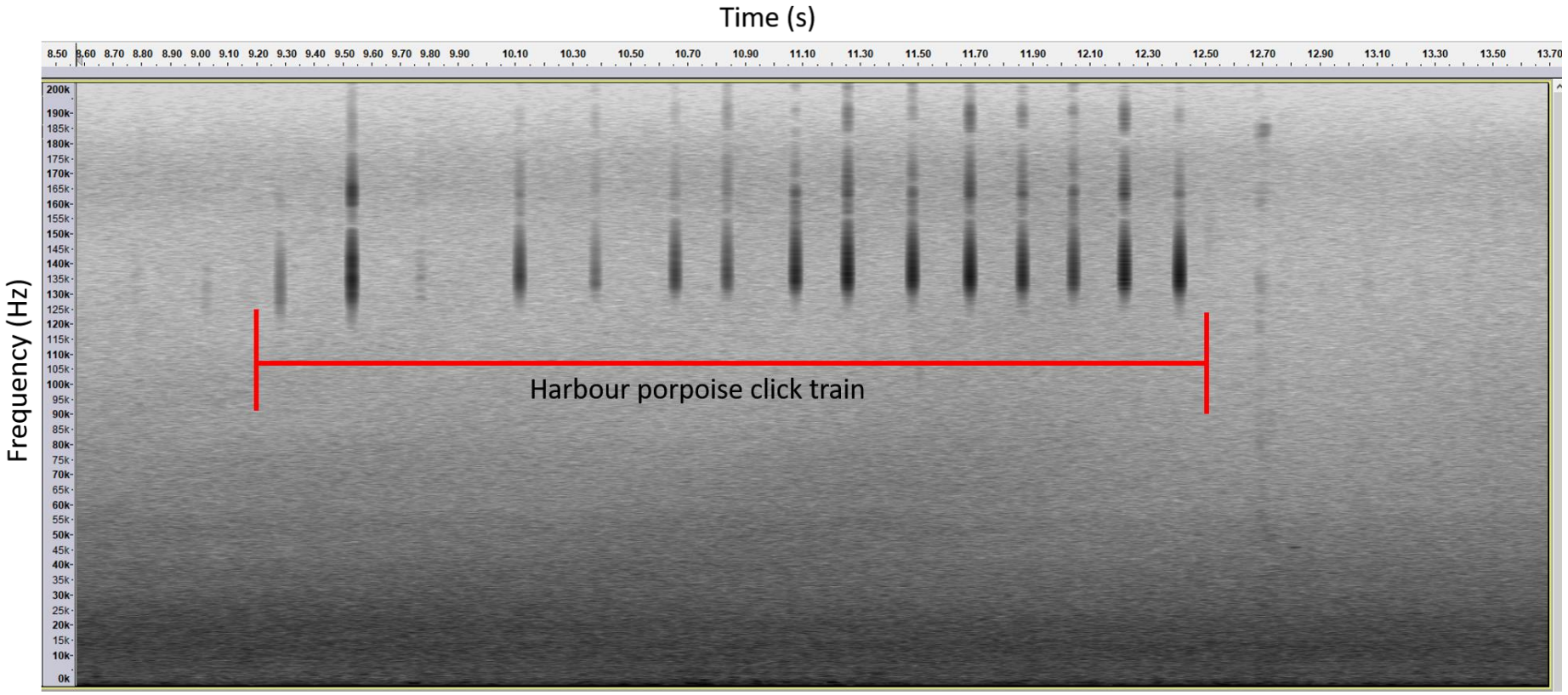

Figure 4. Example spectrogram generated using Audacity (2017) and data collected with an icListenHF hydrophone mounted on a drifter in Minas Passage, at 1300h on October 7th, 2016. A harbour porpoise click train is evident at 120-140 kHz between 9.20 to 12.50 seconds.

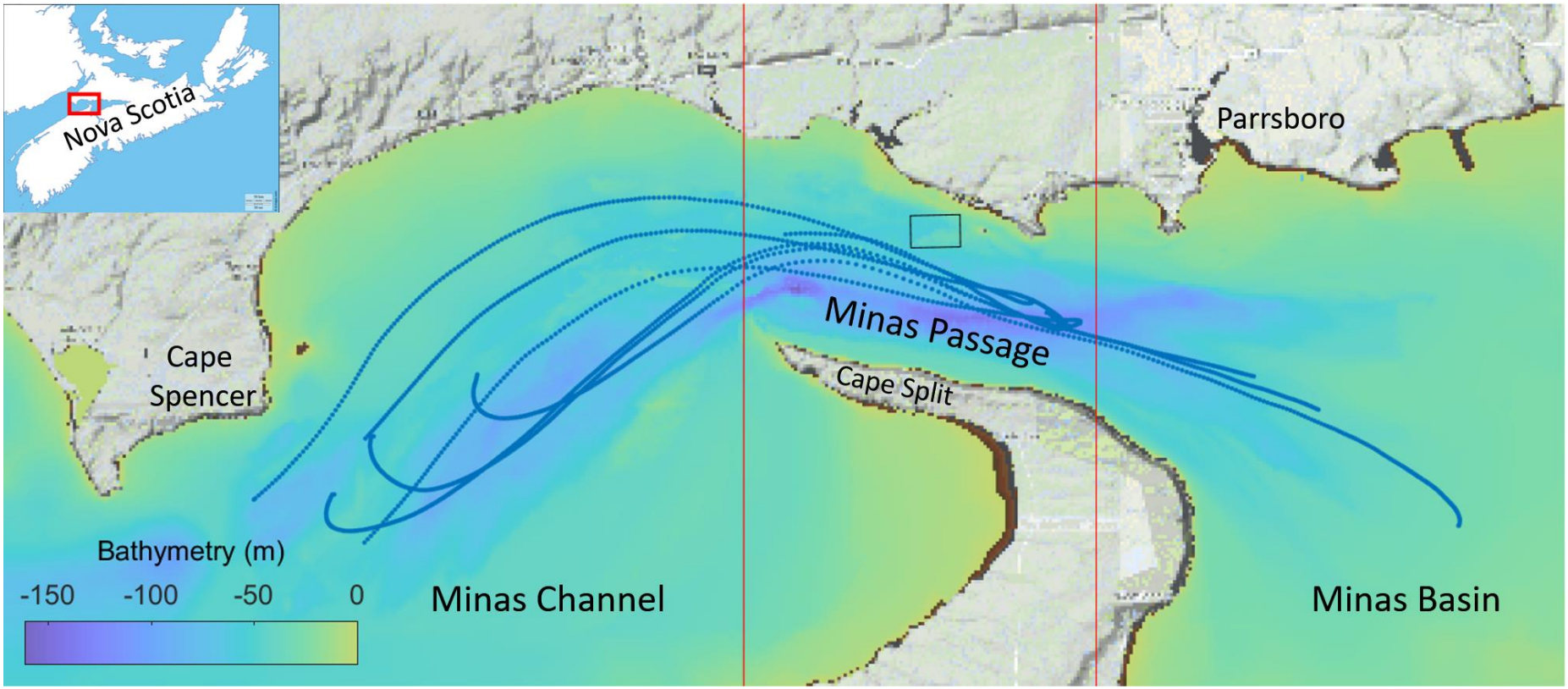

Figure 5. Map of study area, showing six GPS tracks (blue lines) of the drifting hydrophone array during June 12th, 14th, 15th, 16th, 26th and 27th, 2017. Longitude bin edges used for analysis of spatial (left to right: Minas Channel, Minas Passage, and Minas Basin) distribution of porpoise detections are denoted by the vertical orange lines. The FORCE crown lease area is represented by the black box in Minas Passage.

A

B

Figure 6. A) Computer generated image of the Cape Sharp Tidal Turbine (16m diameter rotor) that was operational at FORCE during November 2017 – June 2017 and removed during the drifter study (Cape Sharp Tidal 2017). B) Vessels involved in the turbine removal operation on June 15th, 2017. Note the recovered turbine on the barge. Photo credit: Mike Adams

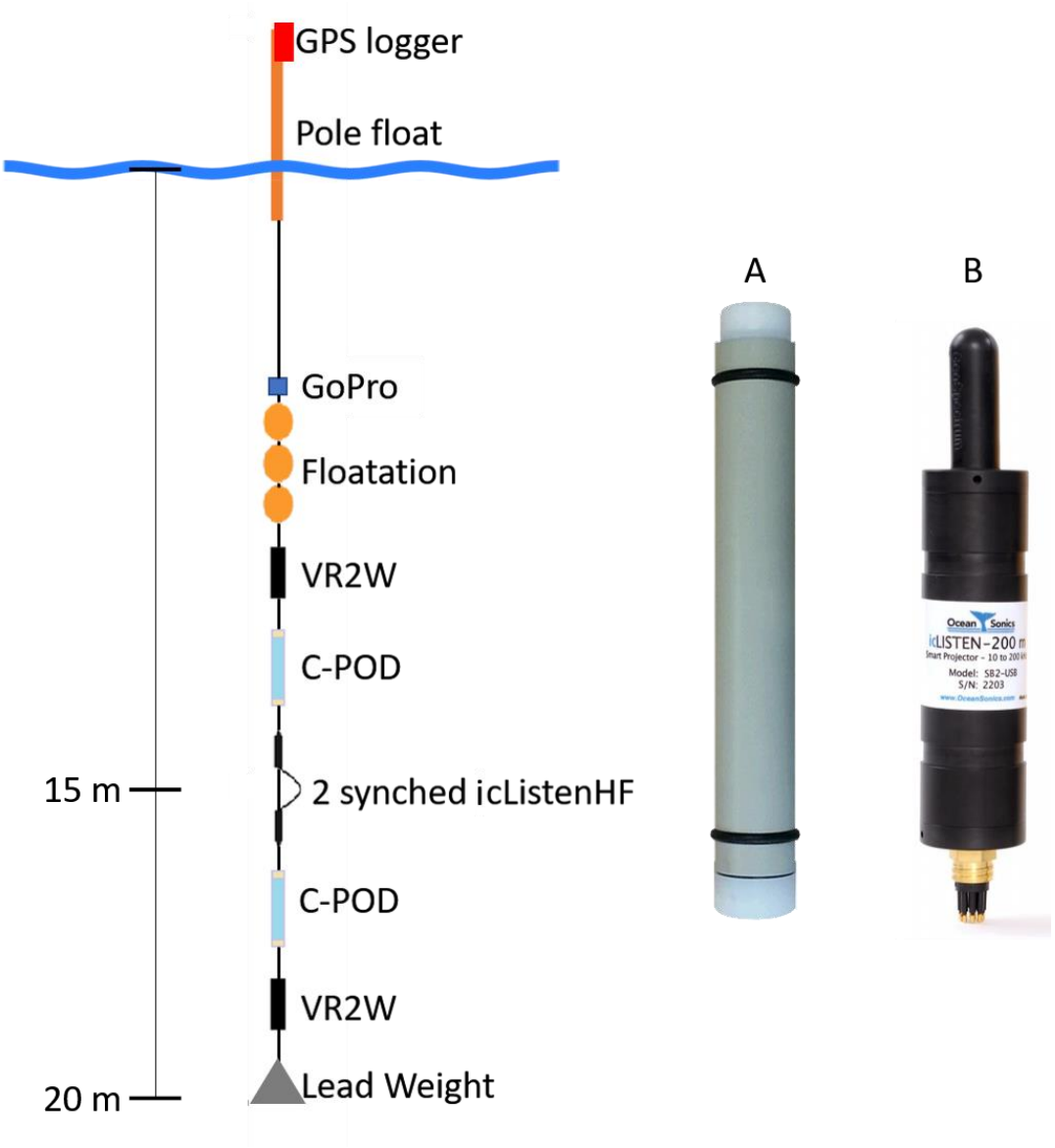

Figure 7. Computer generated schematic of custom-built drifter with full instrumentation loadout. Drifter was deployed in Minas Passage and adjacent areas in June 2017 to collect acoustic data. The icListenHF hydrophones and C-PODS recorded harbour porpoise echolocation activity while the VR2Ws (VEMCO) recorded acoustically tagged fish. Pictured right: A) C-POD, B) icListenHF.

Figure 8. Map of study area, with harbour porpoise detections during drifts through Minas Channel, Passage and Basin, on June 12th, 14th, 15th, 16th, 26th and 27th, 2017. Acoustic detections are represented by the orange (icListenHF 1239) and blue (icListenHF 1211) points. Visual detections are represented by the black asterisks.

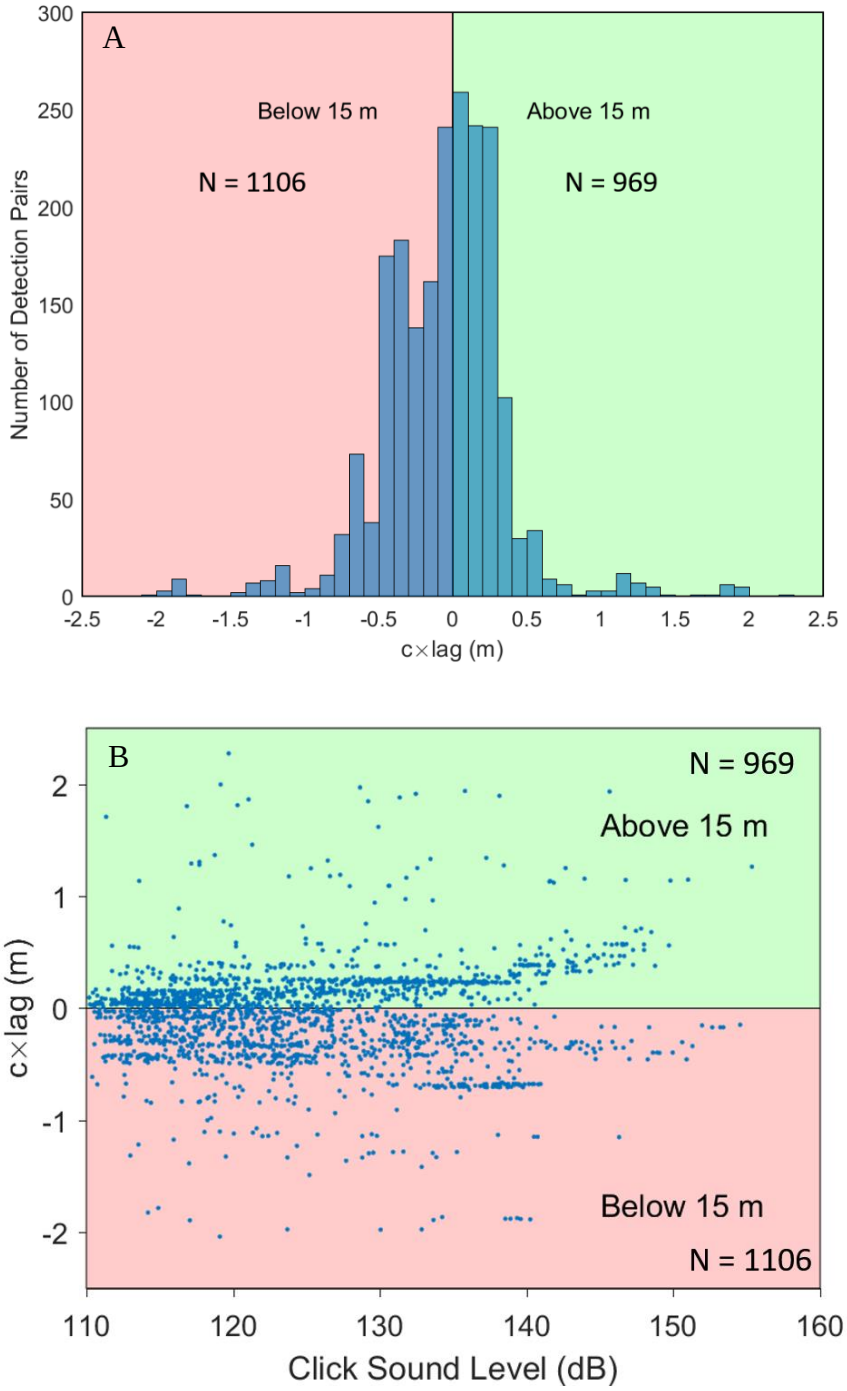

Figure 9. Harbour porpoise depth distribution generated from the lag times of click detection pairs collected in Minas Passage and adjacent areas, during June 2017. Data collected using a drifter with hydrophones mounted at 14 m and 16 m depth (see Figure 7). Lag time is the difference in arrival time of a click received by both the lower and upper hydrophones. Lag = arrival @ lower – arrival @ upper. The lag times were plotted on the X-axis by multiplying by c ~ 1500 m/s (speed of sound in water) as a scaling factor. The red and green shading demonstrates when a paired click was generated below or above the midpoint of the array (15 m) respectively. N = number of paired clicks. A) Histogram demonstrates the distribution of clicks in relation to 15 m depth. B) Scatterplot demonstrates the same distribution but with click sound level (dB).

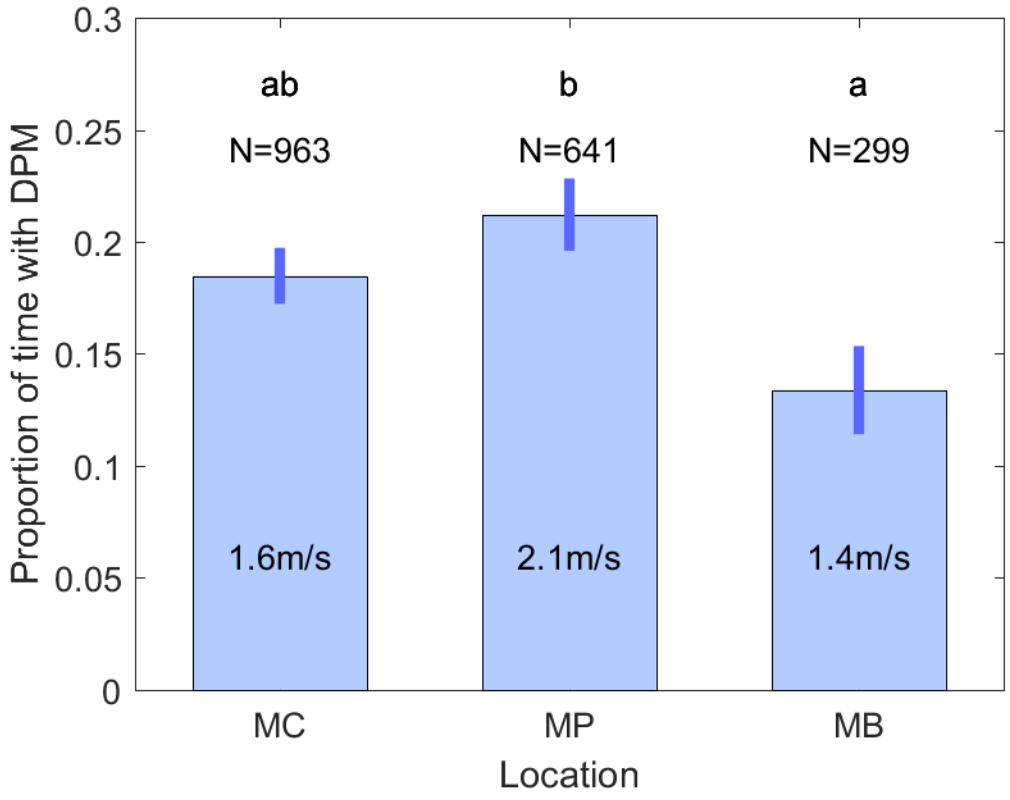

Figure 10. Proportion (mean ± 1 standard error) of time (minutes) with icListenHF Detection Positive Minutes (DPM), as a function of location, integrated across tidal phase and time. Locations: Minas Channel (MC), Minas Passage (MP), and Minas Basin (MB). N equals the number of minutes sampled in each location. Vertical lines on the main bars represent ± 1 standard error. Letters above the bars (a,b) represent post-hoc analysis results (Pairwise Nominal Independence) of a Chi-Squared test. Text within each bar is the average current speed (m/s) for each bin.

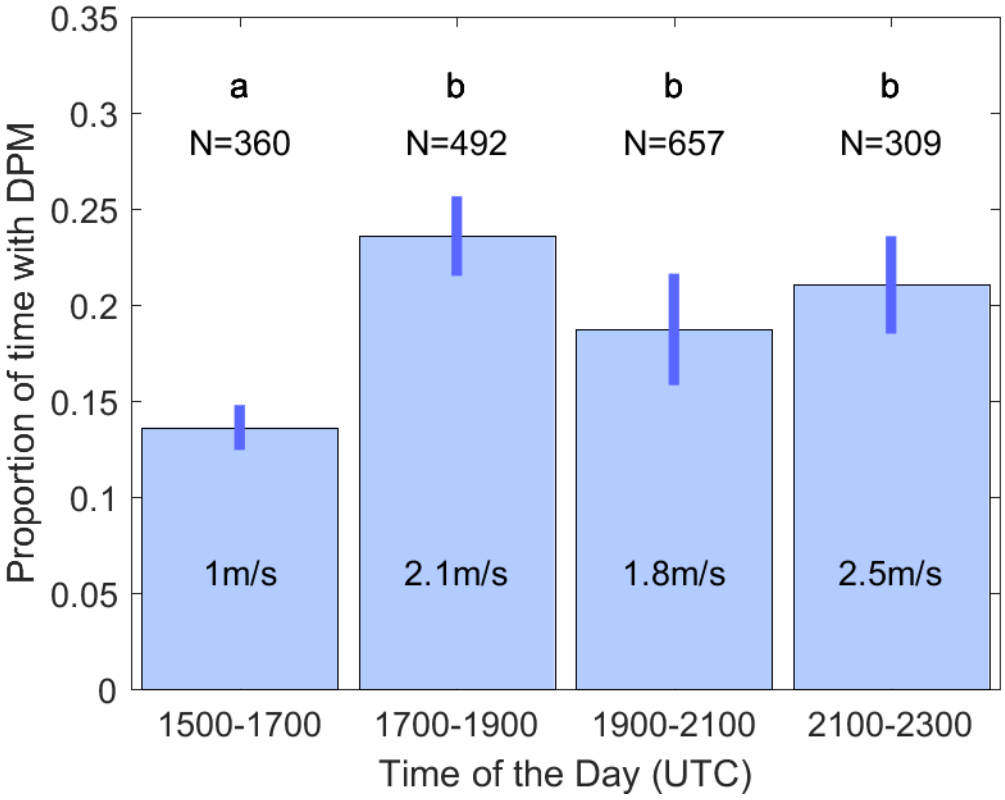

Figure 11. Proportion (mean ± 1 standard error) of time (minutes) with icListenHF Detection Positive Minutes (DPM), as a function of time of day, integrated across tidal phase and location. N equals the number of minutes sampled in each time bin. Vertical lines on the main bars represent ± 1 standard error. Letters above the bars (a,b) represent post-hoc analysis results (Pairwise Nominal Independence) of a Chi-Squared test. Text within each bar is the average current speed for each bin.

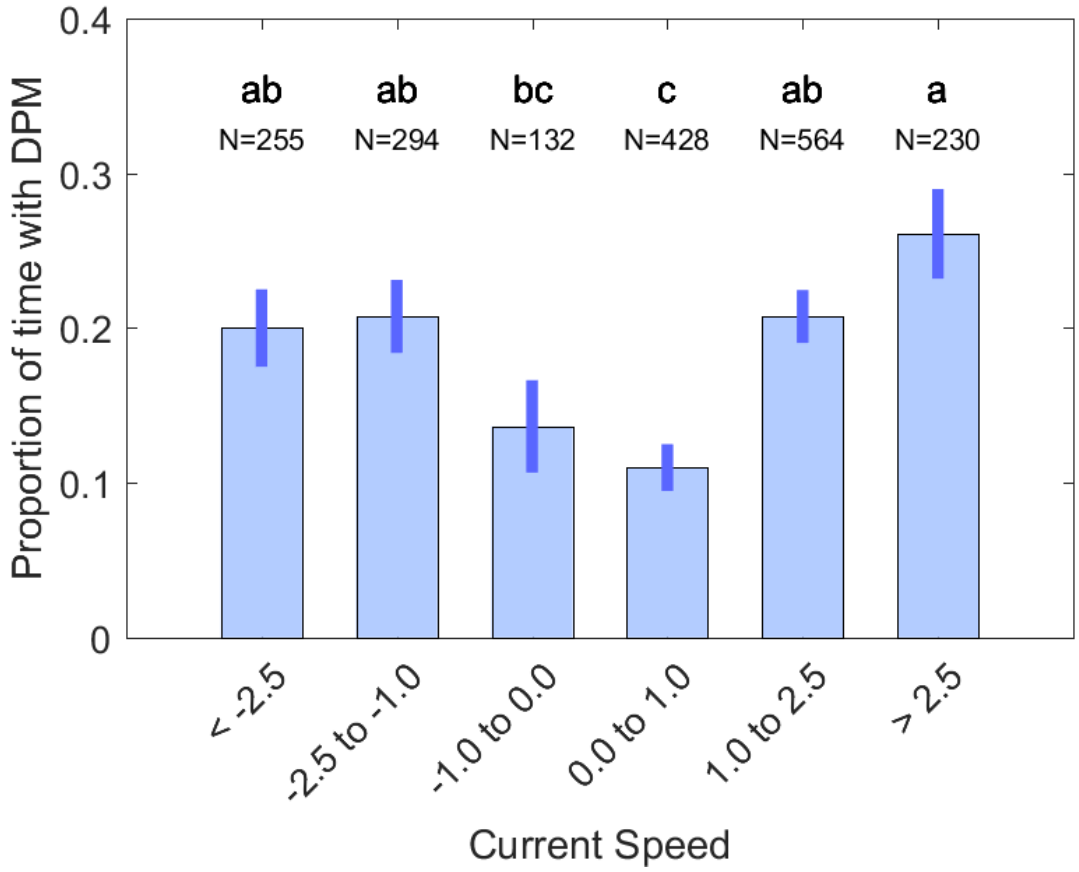

Figure 12. Proportion (mean ± 1 standard error) of time (minutes) with icListenHF Detection Positive Minutes (DPM), as a function of current speed, integrated across time of day and location. Positive current speeds denote flood tide and negative current speeds denote ebb tide. N equals the number of minutes sampled in each current speed bin. Vertical lines on the main bars represent ± 1 standard error Letters above the bars (a,b,c) represent post-hoc analysis results (Pairwise Nominal Independence) of a Chi-Squared test.

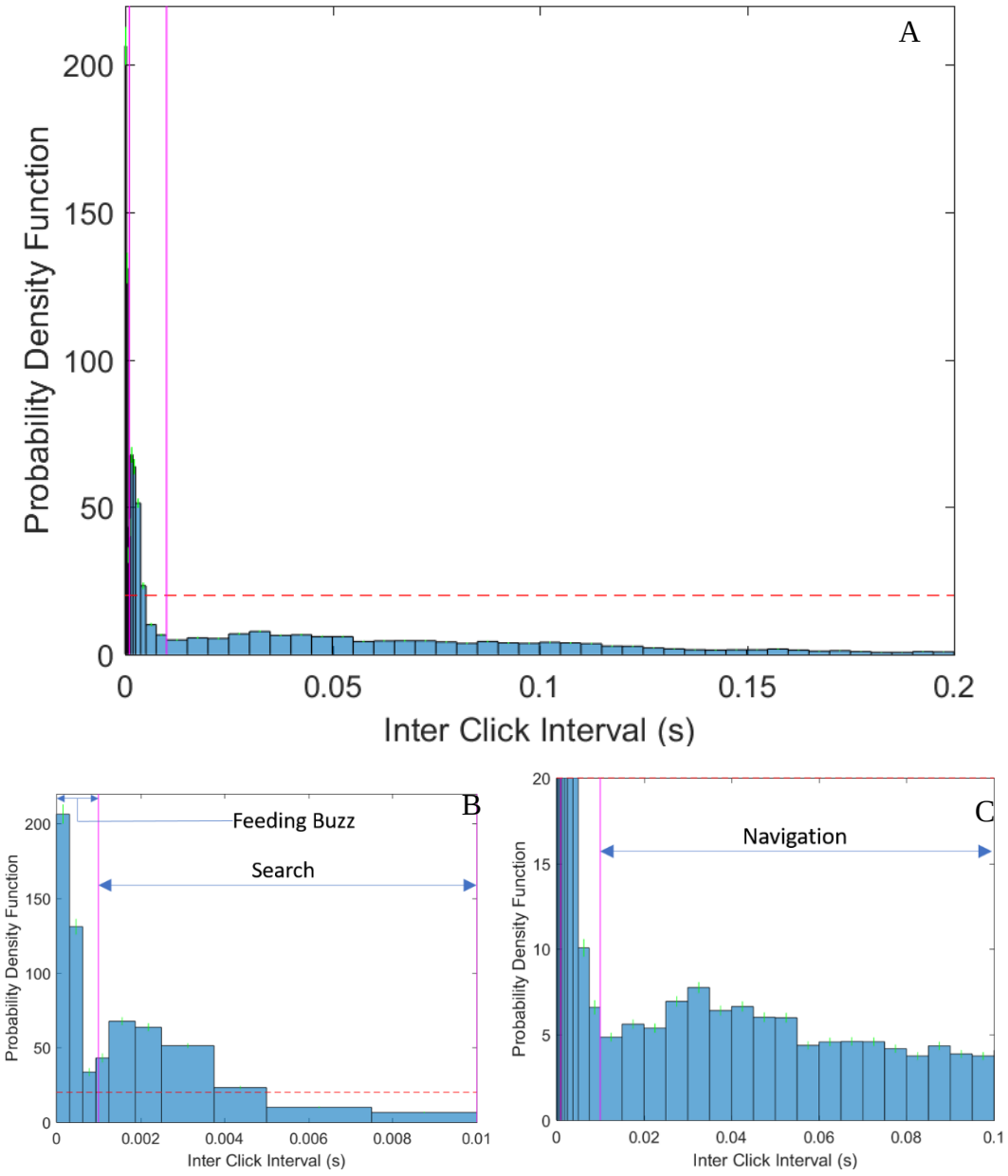

Figure 13. Histograms of the probability density function (with standard deviation bars) used to inspect the range of inter-click intervals (ICI) within the June 2017 acoustic data set collected by the drifting hydrophone array. The histograms were generated using 14851 ICI values. A) ICI range from 0 to 0.2 seconds and a y-axis with values up to 220 which present the entire range of ICI collected. B) ICI range from 0 to 0.01 seconds and a y-axis with values up to 220, highlighting the two modes of the ICI which correspond with search and feeding buzz behaviours. C) ICI range from 0 to 0.1 seconds and a y-axis with values up to 20, highlighting the mode in the ICI which corresponds with navigation behaviour.

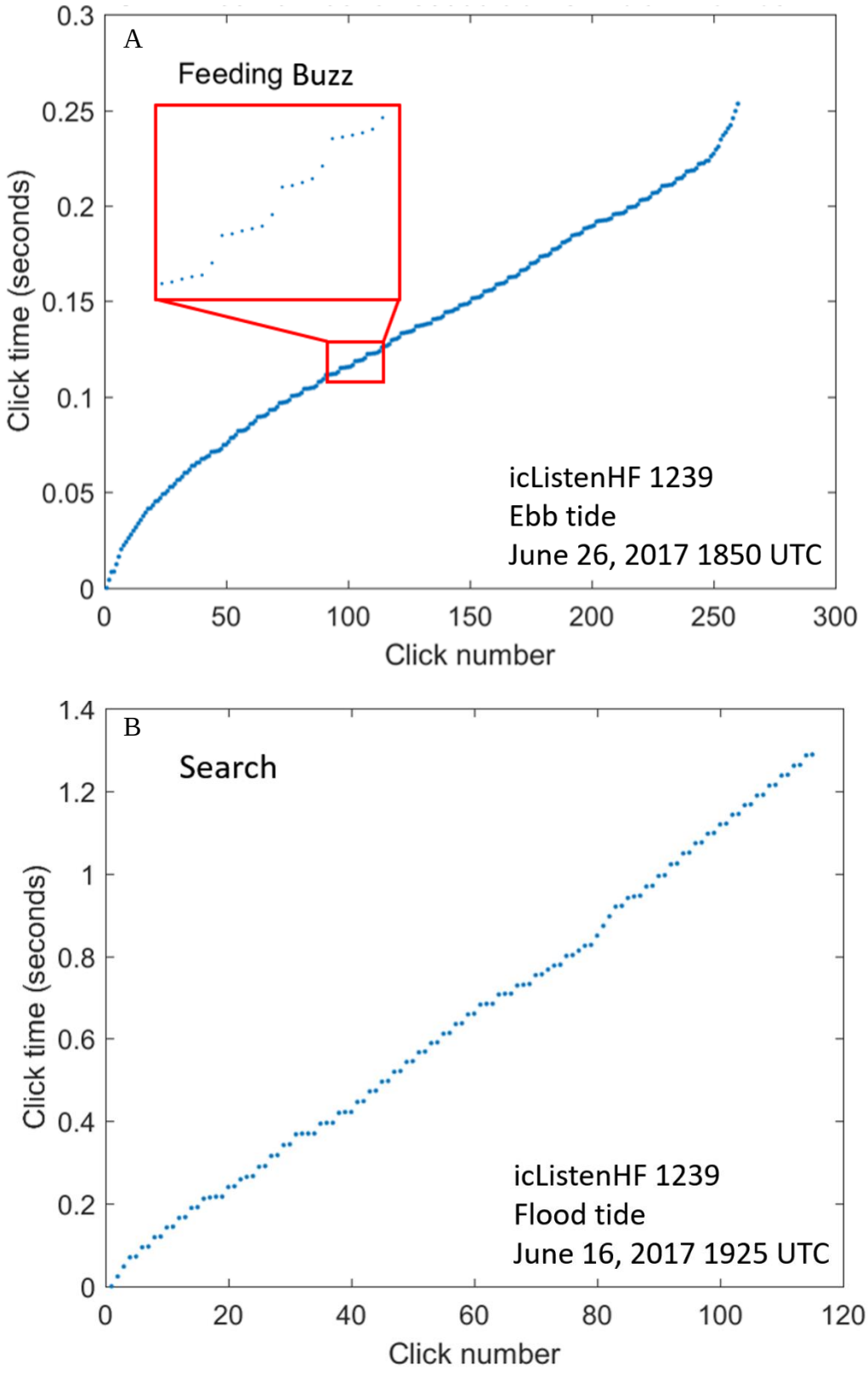

Figure 14. Harbour porpoise behavior based on grouped patterns within click sequences. A) feeding buzz, B) search train. Clicks were detected within the acoustic data collected by a drifting hydrophone array deployed in Minas Passage and adjacent areas during June 2017.

APPENDIX I. DYNAMICS OF SOUND IN THE OCEAN

A1.1 Plane Wave Description

A simple description of sound is a plane wave that moves uniformly in one direction. For a plane wave moving in the positive *x* direction the equations describing pressure *p* and velocity *u* are

$$p = p_a \sin\frac{2\pi}{L}(x - ct) \quad \text{(Eq. A1)}$$

$$u = \frac{p_a}{c\rho} \sin\frac{2\pi}{L}(x - ct) \quad \text{(Eq. A2)}$$

where p_a is the amplitude of the pressure signal, *l* is wavelength, *c* is wave speed, and ρ is density of the medium (henceforth water). This sinusoidal plane wave is illustrated in Figure A1. Note here, we have described the wave as a sinusoid but sound can propagate as any other sufficiently smooth functional form.

For an observer at a fixed point the sound wave will pass by at speed *c*. Thus, the observer will see a complete oscillation in a time $T = l/c$ [s]. This time is called the wave period. The frequency at which wave passes is the reciprocal of wave period and is given the symbol *f* and units of Hz [1/s].

In Figure A1, the gradient of pressure across a small volume of water will apply a net force to that water volume thereby accelerating it according to Newton's $F = ma$ law. In this way the pattern of *u* is changed with respect to time. The gradients in *u* cause patterns of compression and rarefaction that slightly change density and associated pressure. In water, sound propagates at speed *c* of about 1500 m/s. The density of seawater ρ is about 1024 kg/m^3. The amplitude of water motion *u* is therefore only about 10^{-6} m/s for a sound wave with pressure amplitude p_a of 1 Pa.

Although water velocity *u* is very small, the whole pattern (wave form) of *u* and *p* moves much faster, at the speed of sound *c*.

A sound wave causes no overall water mass displacement. On the other hand, the energy of the sound wave propagates at speed *c*. Obtaining the speed of sound requires consideration of thermodynamics. Medwin (1976) proposed a semi-empirical formulation:

$$c = 1449.2 + 4.6T - 0.055T^2 + \quad \text{(Eq. A3)}$$

$$0.00029T^3 + (1.34 - 0.01T)(S - 35) + 0.016z$$

that applies well for our purposes. Here *S* [psu] is salinity, *T* [°C] is temperature and *z* [m] is depth.

A1.2 Attenuation

Linear friction (molecular effects) contributed mainly by boric acid, magnesium sulphate and pure water will cause wave amplitude to decline as it propagates (Francois and Garrison 1982a&b). Thus, if the amplitude was p_a at time *t = 0* then the pressure equation for a plane wave becomes

$$p = p_a \exp(-\beta t) \sin\frac{2\pi}{L}(x - ct) \quad \text{(Eq. A4)}$$

where the coefficient of attenuation β is also the coefficient of linear friction. The water velocity *u* also decays in the same exponential manner.

A1.3 Point Source (Radial Spreading)

Strictly speaking porpoises and many other sound sources in the ocean (but not all sound sources) are dipoles but beyond a small distance from the source the sound

can be considered as though it is spreading radially from a point source. For a porpoise the radial spreading is mostly confined within a ~16° beam (Au 1999). The cross-sectional area of a beam (or sphere for the omnidirectional case) increases as the square of radial distance from the source r^2. Thus, the energy in the wave is spread over an increasing area as the wave propagates away from its source. This is called radial spreading.

Acoustic intensity is defined as *pu* and represents the rate at which sound energy passes through a unit area. In the following we will follow the common convention of working with pressure intensity I [Pa^2] which is defined as the mean square pressure.

Taking account of both radial spreading and attenuation with distance from the source the equation for intensity I can be written

$$I = I_0 \frac{\exp(-2a(r-r_{\mathrm{ref}}))}{(r/r_{\mathrm{ref}})^2} \qquad \text{(Eq. A5)}$$

where $a = \beta/c$ and I_0 is pressure intensity at the reference range r_{ref}. The convention is to calibrate for a reference range $r_{\mathrm{ref}} = 1$ m. Note there are two reasons for working with respect to a reference range. First, many sound sources are dipoles (including the phonic lips of porpoises) and the above equation is inappropriate when close to dipoles. Second, the intensity of a point source tends to an unphysical value (infinity) at $r = 0$.

A1.4 Decibels

Decibels are the biological scale for perception of sound intensity I. The convention for sound propagating in water is to set the reference value for sound pressure p_{ref} to 10^{-6} Pa. Thus, the reference for intensity I_{ref} is 10^{-12} Pa^2. Hearing tends

to be logarithmic so a sound with ten times the intensity is perceived (sensed) as being twice as loud. Thus, we introduce the sound pressure level *L* in decibels as the following transformed value of intensity.

$$L = 10 \log_{10} \frac{I}{I_{\text{ref}}} \qquad \text{(Eq. A6)}$$

The unit for *L* is decibel and it is given the symbol dB. At frequencies near 100 kHz the threshold level for porpoise hearing is about 35 dB (Kastelein *et al.* 2002, Figure 2). Substituting the attenuation and radial spreading equation (Eq. A5) into Eq. A6 we obtain

$$L = L_0 - 20 \log_{10} \left(\frac{r}{r_{\text{ref}}}\right) - \alpha(r - r_{\text{ref}}) \qquad \text{(Eq. A7)}$$

where $L_0 = 10 \log_{10} I_0$ is the source pressure level, $20 \log_{10} (r/r_{\text{ref}})$ is the pressure level decline due to radial spreading, and $\alpha = a20 \log_{10} (e)$ is the seawater absorption coefficient for sound energy. Figure A2 shows how the level of a porpoise click (L_0 = *172* dB) drops with range due to radial spreading and the combined effects of radial spreading and absorption.

Various semi-empirical formulations are available for α (Fisher and Simmons 1977; Francois and Garrison 1982a&b; Ainslie and McColm 1998). Generally, α is a function of frequency *f*, salinity *S*, temperature *T*, and depth *z*. For example, for near surface porpoise clicks (*f = 130* kHz, *z = 10* m), when *S = 34* psu and *T = 8* °C, α = 37.5 dB/km.

The intensity of sounds in nature varies over many orders of magnitude. It should not therefore be surprising that organisms evolved to hear on a logarithmic scale. Also, sounds span a wide range of frequencies. It is therefore no coincidence that a geometric scale also applies to how organisms hear frequency (Varshney and

Sun 2013). Consequently, the octave scale is commonly used in music. For example, a 4 kHz sound is heard as having twice the pitch of a 2 kHz sound. It would make just as much sense to log transform frequency as it does intensity, but the usual scientific convention is to work with Hz and to plot frequency on a log scale.

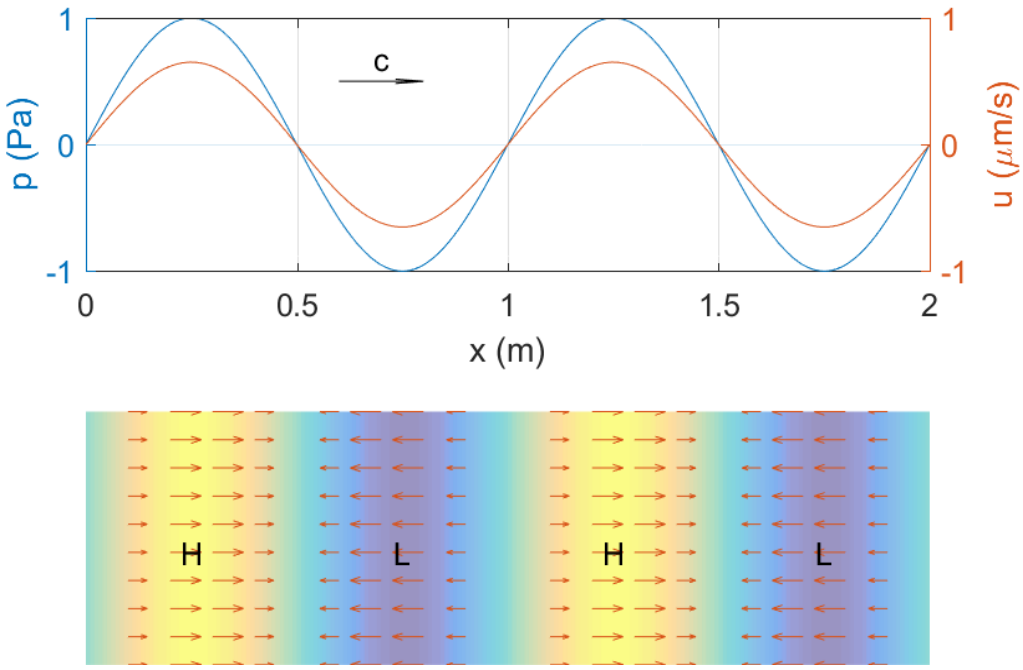

Figure A1. Pressure gradient of plane wave propagation. H = High pressure, L = Low pressure, c = speed of sound. Source: Brian Sanderson.

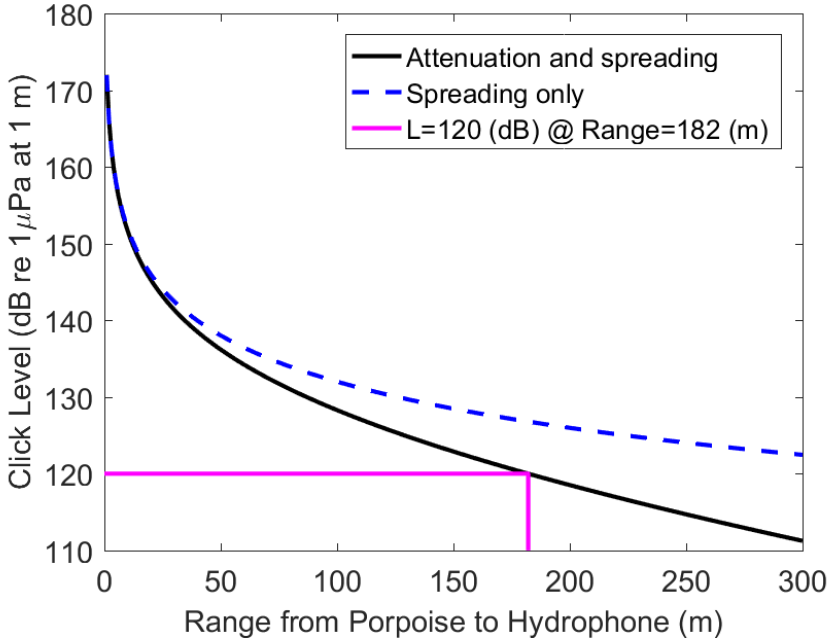

Figure A2. Modelled decrease in porpoise click sound level due to attenuation and spreading and spreading only. The frequency and source level of the modelled click are 130kHz and 172 dB re1µPa@1m. The pink lines indicate that at 182m from the receiver the click sound level received in 120 dB. This assumes maximum theoretical porpoise click source level (172 dB re1µPa@1m). Source: Brian Sanderson.

APPENDIX II. DPM PROPORTION ACROSS LOCATION, TIME OF DAY, AND CURRENT SPEED

Table A1. Three - dimensional array of proportions of DPM across location, time of day, and current speed. Time of day is in UTC and current speed is in m/s where a positive current speed is the flood tide and a negative is the ebb tide. *p* = proportion of DPM, *SE* = standard error, and N = number of minutes sampled.

Current Speed (m/s)	Time of Day (hours)	Location					
		Minas Channel *p (SE)*	N	Minas Passage *p (SE)*	N	Minas Basin *p (SE)*	N
-4.10 to -2.50	1500-1700	Na(Na)	0	Na(Na)	0	Na(Na)	0
	1700-1900	Na(Na)	0	Na(Na)	0	Na(Na)	0
	1900-2100	0.42 (0.09)	31	0.12 (0.04)	84	Na(Na)	0
	2100-2300	0.20 (0.04)	117	0.22 (0.09)	23	Na(Na)	0
-2.50 to -1.00	1500-1700	Na(Na)	0	Na(Na)	0	Na(Na)	0
	1700-1900	Na(Na)	0	Na(Na)	0	Na(Na)	0
	1900-2100	0.26 (0.09)	23	0.15 (0.03)	118	Na(Na)	0
	2100-2300	0.24 (0.03)	153	Na(Na)	0	Na(Na)	0
-1.00 to 0.00	1500-1700	0.00 (0.00)	18	Na(Na)	0	Na(Na)	0
	1700-1900	Na(Na)	0	0.25 (0.09)	24	Na(Na)	0
	1900-2100	Na(Na)	0	0.23 (0.06)	52	0.00 (0.00)	13
	2100-2300	Na(Na)	0	Na(Na)	0	Na(Na)	0
0.00 to 1.00	1500-1700	0.10 (0.02)	211	Na(Na)	0	Na(Na)	0
	1700-1900	Na(Na)	0	0.18 (0.06)	49	Na(Na)	0
	1900-2100	Na(Na)	0	0.41 (0.08)	39	0.00 (0.00)	65
	2100-2300	Na(Na)	0	Na(Na)	0	0.00 (0.00)	4
1.00 to 2.50	1500-1700	0.20 (0.04)	119	Na(Na)	0	Na(Na)	0
	1700-1900	0.27 (0.03)	172	0.07 (0.05)	28	0.16 (0.05)	49
	1900-2100	Na(Na)	0	0.09 (0.04)	44	0.23 (0.04)	140
	2100-2300	Na(Na)	0	Na(Na)	0	0.00 (0.00)	12
2.50 to 4.60	1500-1700	0.40 (0.15)	10	0.00(0.00)	2	Na(Na)	0
	1700-1900	0.11 (0.07)	18	0.31 (0.04)	136	0.00 (0.00)	16
	1900-2100	0.00 (0.00)	6	0.29 (0.07)	42	Na(Na)	0
	2100-2300	Na(Na)	0	Na(Na)	0	Na(Na)	0

APPENDIX III. MODELLED VERTICAL ERROR ASSOCIATED WITH PORPOISE DEPTH DISTRIBUTION

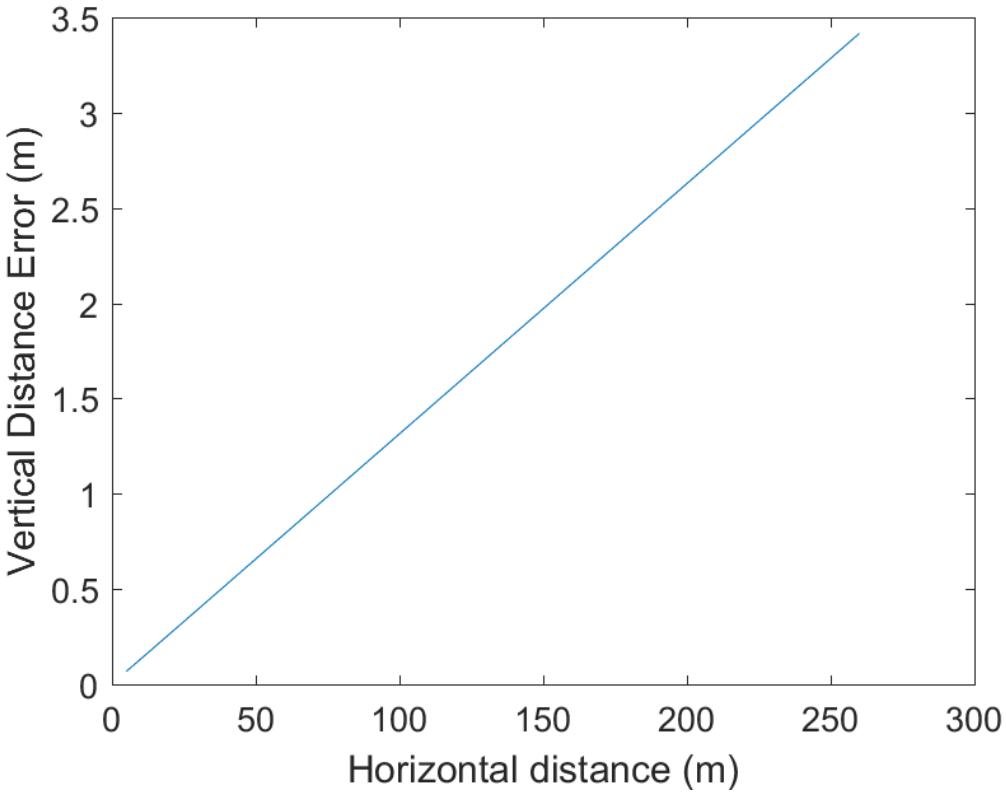

Figure A3. Modelled vertical distance error (m) in porpoise depth distribution due to the error in the calculated lag times in click detection between the two hydrophones (19.5μs) for a click produced at different ranges (m) from the array.